Scholar Commons
USF University of South Florida

University of South Florida
Scholar Commons

Graduate Theses and Dissertations | Graduate School

10-25-2010

Capillary Self-Assembly and its Application to Thermoelectric Coolers

James K. Tuckerman
University of South Florida

Follow this and additional works at: http://scholarcommons.usf.edu/etd

 Part of the American Studies Commons

Scholar Commons Citation

Tuckerman, James K., "Capillary Self-Assembly and its Application to Thermoelectric Coolers" (2010). *Graduate Theses and Dissertations.*
http://scholarcommons.usf.edu/etd/3704

This Thesis is brought to you for free and open access by the Graduate School at Scholar Commons. It has been accepted for inclusion in Graduate Theses and Dissertations by an authorized administrator of Scholar Commons. For more information, please contact scholarcommons@usf.edu.

www.manaraa.com

Capillary Self-Assembly and its Application to Thermoelectric Coolers

by

James K. Tuckerman

A thesis submitted in partial fulfillment
of the requirements for the degree of
Master of Science in Mechanical Engineering
Department of Mechanical Engineering
College of Engineering
University of South Florida

Major Professor: Nathan Crane, Ph.D.
Craig Lusk, Ph.D.
Kyle Reed, Ph.D.

Date of Approval:
October 25, 2010

Keywords: Solder, Peltier Cooling, Surface Tension,
Interfacial Energy, Energy Minimization

Copyright © 2010, James K. Tuckerman

www.manaraa.com

Table of Contents

www.manaraa.com

www.manaraa.com

List of Tables

www.manaraa.com

List of Figures

www.manaraa.com

www.manaraa.com

Abstract

The thermoelectric effect was discovered well over a century ago, yet performance has not shown improvement until recent years. Prior work has shown that the thermoelectric effect can be enhanced by the use of microscale pieces of thermoelectric material. Conventional assembly techniques are inadequate to deal with parts of this size, making it necessary to find a suitable alternative before these devices can be made economically. Capillary self-assembly is a promising alternative to conventional techniques. This method employs the use of preparing substrates with areas of favorable surface tension to place and align parts. Still, many obstacles have to be overcome to adapt this process for use of constructing thermoelectric coolers. The goal of this work is to overcome these obstacles and assess the viability of self-assembly for fabricating these devices. In effort to make the method more effective a process for creating more uniform deposits of solder is also assessed. This work shows that microscale thermoelectric elements can be assembled into functional thermoelectric devices using self-assembly techniques through the assembly of coolers in experimental work.

www.manaraa.com

Chapter 1 - Introduction

1.1 Basics of Thermoelectric Coolers

In 1821, Johan Seebeck discovered the thermoelectric phenomenon. Later, in 1834, scientific understanding of the phenomenon was refined by Jean Charles Peltier. Thermoelectric coolers are made from specialized materials that are capable of producing a heat flux in the presence of an applied current. In order to do this, they must have a collection of positive and negatively doped elements. These coolers have the potential to provide a low-voltage solid-state cooling device. Because they are so small and contain no moving parts, they are optimal devices for electronics and telecommunications applications where large amounts of heat are generated in small spaces, and for applications requiring gravity independence.

Thermoelectric coolers can also function for power generation in the presence of a temperature difference; they have already been used in deep space probes for this application. Their use in future applications is highly dependent on increasing their efficiency and making them more compatible with compression refrigeration.

www.manaraa.com

1.2 Increasing Thermoelectric Cooler Efficiency

While thermoelectric theory was developed almost two centuries ago, little progress toward improved efficiency had been seen up until the last 15 years. Increasing the efficiency of thermoelectric cooling is the primary goal of assembling these coolers. Recently low-dimensional thermoelectric materials have been found to be promising candidates for dramatically increasing thermoelectric cooler performance. [1, 2] These materials are largely superior due to their reduced thermal transport rates as thermal transport is inversely proportional to cooler efficiency. A more detailed review of thermoelectric cooler efficeincy will be covered later in this thesis in chapter 2. The problem in increasing efficiency by decreasing size is that traditional pick-and-place assembly methods are incapable of performing these assemblies at practical rates and costs due to the large numbers of microscale components needing high-precision positioning [3]. This is where the need for a new self-assembly technique arises, and self assembling looks promising for providing the needed large-scale batch processing with the required high precision.

1.3 Self-Assembly

Self-assembly is a broad term referring to any process that produces an ordered system from disordered parts without each part being specifically placed at an exact location. The process is abundant in nature and provides the basis for all manner of structures from the formation of crystals to protein folding [4, 5].

www.manaraa.com

Research on self-assembly in research involves a wide spectrum of techniques to solve the challenges in creating a plethora of different devices. These methods can be divided into two major categories: those involving the self-assembly of structures and those involving wafer-to-wafer transfer of self assembled components. The latter is the primary concern of this thesis. Nevertheless, other assemblies will be reviewed as they are pertinent to the creation of self-assembled thermoelectric coolers.

1.3.1 Solder-Based Self-Assembly Transfer Process

Based on previous work done by Crane *et al.* [6], solder-based assemblies would be ideal for assembling thermoelectric coolers. They have outlined a method by which the two different materials can be assembled on a temporary substrate and transferred to the final device. The process starts by attaching the individual elements to an intermediate substrate. This process step is done in two steps so that only one type of element is assembled at a time avoiding the necessity of defining different binding conditions for the different element types. The parts are then transferred onto the final substrate in two separate transfer processes. The final step brings in a top substrate to complete the electrical connection. This same method is used, with some modification to the materials and size scales, for this work. The process is summarized in Figure 1.

www.manaraa.com

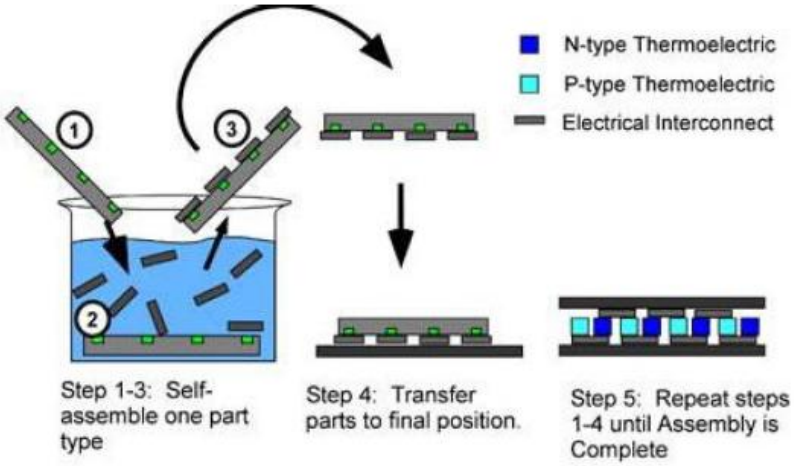

Figure 1: Multi-stage assembly outlined by Crane *et al.*[6] The process involves two major stages, assembling parts on a temporary substrate and then transferring parts to the final substrate.

1.4 Topics to be Addressed in Thesis

This thesis describes a method of assembling thermoelectric coolers using capillary self-assembly, using the method developed by Crane *et al.* The research focused on finding appropriate materials and assembly conditions, including site geometry (including additional supports for orientation if necessary), fluid volumes, assembly fluid, fluxing agents, and binding fluids. The binding fluids were limited to solder based assemblies and the fluxing agents were acids. Their strength and quantity were determined in this research.

www.manaraa.com

Chapter 2 - Literature Review

Several issues are examined in this literature review. First, works involving the motivation behind the self-assembly of TECs are reviewed. This includes basic history of thermoelectric cooling and the state of the art for their performance. Then a series of methods for assembling microscale elements are examined. Several methods are examined, which may not be viable at the element sizes currently being assembled. They still provide valuable information about the nature of surface tension based self-assembly. As the size scales of these assemblies is reduced as planned in future work, these methods of assembly will also become usable. The relation of each work is briefly summarized below in Table 1.

Table 1: Table summarizing the different techniques researched for self-assembly of TECs.

Process	Forces	Relation to TEC Assembly	Reference
Nanoscale Assembly	Gibbs and Helmholtz free energy, Van der Waals, electrostatic and magnetic	Little relation to microscale assembly though, assembly of nanowire TECs is a possibility for future investigation	15-19
Electrostatic	Electrostatic charging	Forces are too small to assemble the current assembly sizes, but future assemblies could be aided by the use of electrostatic forces as the parts are metallic	11,15,20
Chemical	Chemical bond (bridging flocculation)	This is a novel concept for creating assemblies, but without a chemical agent which specifically will bond two metallic surfaces it does not offer a solution for TEC assembly	13

www.manaraa.com

Table 1 (Continued)

Van der Waals	Van der Waals surface bonding	One of the earliest forces used for self-assembly as no modification if necessary so long as the faces being assembled are smooth. The ends of our thermoelectric elements are not, but could be made so in the future.	14,20
Capillary (SAM)	Capillary forces created by patterning of hydrophobic monolayer's on hydrophilic surfaces	This is the most prevalent form of capillary self-assembly since the hydrophobic sites are easily coated with lubricant for assembly. While the forces provided by the lubricant are smaller than those of solder based assembly the energy minimums can be reached easier due to the decrease in corrective forces needed with use of the lubricants.	3,23,27-30
Capillary (Solder)	Capillary forces created by solder and an ambient fluid interface	Several examples exist of solder being used to drive assembly processes for three dimensional electrical networks. These assemblies use the same materials that will be used in TEC assembly to create free form assembly (as opposed to the wafer-to-wafer process). They provide a valuable reference in methods of assembly using these materials.	10,31-35
Capillary (Self-Folding Solder Hinges)	Capillary Forces of solder deposited and then reflowed	This is a very active area of research. While these are not examples of assembly, they do offer a valuable resource of information about how solder volume relates to the equilibrium position of the elements being held by the solder.	40-45

2.1 Thermoelectric Cooling

The basic structure of a thermoelectric cooler is identical to that of thermoelectric generator. By combining two different dopings of certain semiconductor materials as shown in Figure 2,thermo electric generators are

www.manaraa.com

able to produce a voltage potential as the temperature changes. Similarly, thermoelectric devices are typically made using semiconductors. Like other semiconductors, the thermoelectric materials are doped with materials with a specified number of valence electrons. For n-type materials, an element with 5 valence electrons is chosen, which would most likely be antimony; in this case the element will donate an electron to the material.

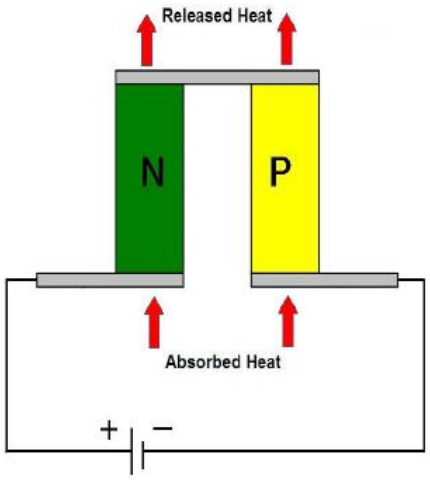

Figure 2: Model of a simple thermoelectric cooler. By providing a voltage potential at the terminals, the flow of electrons through the oppositely doped thermoelectric material will provide a heat flux across the material by absorbing heat from the bottom.

In the case of p-type materials, an element with 3 valance electrons is added; this takes away an electron from the material giving an overall positive charge [7].

The primary material for thermoelectric application near room temperatures is bismuth telluride (Bi_2Te_3). Bismuth telluride is an ideal choice for

www.manaraa.com

thermoelectric cooling because of its wide operating range of -46 to 204°C, making it useful for heating and cooling applications alike. Bismuth telluride is doped with Selenium (n-type) and Antimony (p-type). The doping of bismuth telluride alters its thermoelectric properties; the n-type material has a maximum temperature difference of 232°C and an efficiency of 13.5%. The p-type material is less than half as efficient, only 5.8%, but it has a maximum temperature difference of 601°C [7].

Other thermoelectric elements include Bismuth-Anitimony alloys, Lead Telluride and Silver-Antimony Telluride. There is no clear winner in efficiency for all cases, but rather the material selection will depend on the temperature of the application for the device. Bismuth Telluride is most commonly used because it is most effective near room temperature. Lead Telluride alloys by comparison are most effective at temperatures over 500 K. While Bismuth-Antimony compounds are only effective from 80 to 300K and Silver Antimony Telluride operates best from 523 to 773 K. The materials are summarized in Table 2 below [8].

Table 2: List of commonly used thermoelectric materials and their zT values for common operating temperatures. [7]

Material	Composition	zT (deg^{-1})	Temperature Range (K)
Bismuth Telluride	Bi_2Te_3	$3.0\text{-}3.3x10^{-3}$	227-477
Lead Telluride	PbTe	$1.2\text{-}15.x10^{-3}$	500-1000
Silver Antimony Telluride	$AgSbTe_2$	$\sim1.8x10^{-3}$	523-773
Bismuth Antimony	Bi-Sb*	$1.8\text{-}5.2x10^{-3}$	80-300

www.manaraa.com

2.1.1 Thermoelectric Cooler Efficiency

The efficiency of thermoelectric coolers is often measured by the nondimensional figure of merit ZT. This figure of merit includes 3 contributing factors, the Seebeck coefficient, S, the suppression of electrical resistivity ρ, and the thermal conductivity, λ, in the relationship given by

$$ZT = \frac{S^2 T}{\rho \lambda} \tag{1}.$$

Typical thermoelectric devices developed in the last century have seen a figure of merit approaching 1.0 [2]. This relationship may also be expressed as a function of electrical conductivity σ, [8,1]

$$ZT = \frac{S^2 \sigma T}{\lambda} \tag{2}.$$

If one assumes that the charge and heat flow are one dimensional, the properties of the thermoelectric material are temperature independent, and if there is no internal electrical resistance, the maximum temperature difference can be expressed as a function of the material property Z [2]

$$\Delta T_{\max} = (T_h - T_C)_{\max} = \frac{Z T_c^2}{2} \tag{3}.$$

This equation is useful when designing coolers for maximum absolute cooling and assumes no internal heat generation.

www.manaraa.com

The composite material property Z used here requires contribution from both the effective Z of the thermoelectric material such that,

$$Z = \frac{(S_p - S_n)}{(\sqrt{\lambda_n \rho_n} + \sqrt{\lambda_p \rho_p})^2} \tag{4}.$$

The length, L, and area, A, are also important to consider when increasing thermoelectric cooler efficiency. The aspect ratios of the n and p type elements must be scaled for optimum temperature drop so that it satisfies the relationship [2],

$$\frac{L_n A_p}{L_p A_n} = \sqrt{\frac{\rho_p \lambda_n}{\rho_n \lambda_p}} \tag{5}.$$

Under these same assumptions an equation relating heat flux to the Seebeck coefficient, electrical resistivity and aspect ratio of the elements being used can be developed. This relationship is found to be

$$q_{\max} = \frac{A}{2L} \frac{S^2}{\rho} T_h^2 \tag{6}.$$

These basic equations have been used to model the efficiency of thermoelectric coolers for over a century. Not until the 1990's when theoretical predictions indicated that newly developed superlattices, nanowire and quantum dots could provide candidates for high performance thermo electric devices were corrections made to this traditional theory [2]. The increase in thermal

www.manaraa.com

performance is due to at least two factors. Dominant vibrations in the lattice structure of materials called phonons are decreased; since phonons are the dominant cause of heat transfer in materials the effective thermal conductivity, λ, is reduced. Secondly due to quantum confinement the electrical conductivity, σ, is increased. The increase in ZT is caused by the inverse relationship with λ, and the direct relationship with σ [2, 8]. Element thickness has a profound effect on efficiency as well as seen in Figure 3.

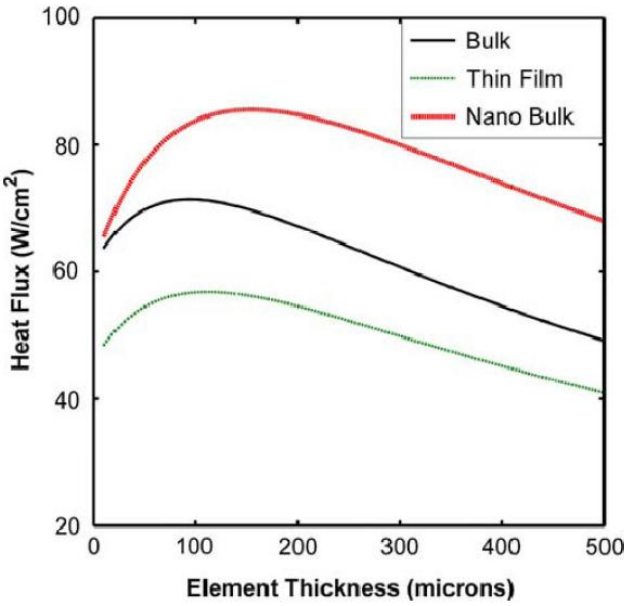

Figure 3: Plot of heat flux capacity vs. element size. Note the improved efficiency of nano sized elements versus a bulk material or thin film (which is largely limited by the thickness that can be manufactured).[6]

Current methods of assembling these coolers involve geometrically constraining the parts. Geometric constraint assembly uses a template to place parts by only allowing them to fall through the template and assembly in one direction. This method leads to using larger aspect ratios, of height to width,

www.manaraa.com

which are required to correctly orient the parts, but which are not necessarily favorable for effective heat transfer. Other methods involve grasping parts, moving them to the desired location, and releasing them. This has several disadvantages in smaller size ranges when the gravitational forces are much smaller in magnitude than Van der Waals, electrostatic and surface tension forces. These forces prevent reliable release of the parts. The use of geometric constraint based assembly can be useful for large batch assembly of micro-sized elements. The drawback of this technique is that the parts need to be geometrically constrained, to define their orientation into assembly sites meaning symmetrically shaped parts will not work. This is because; a difference in geometry must prevent parts from falling into position without a contact facing the substrate. This means to assemble optimal thermoelectric coolers, with small symmetrically-shaped elements, it is necessary to look for a new means of assembly.

It is difficult to assemble elements with larger aspect ratios. This is due to the larger forces seen at the base of the parts as the height of the part increases relative to its width. As shown in Figure 4 the distance to the center of gravity d increases with the height h for the same angle Θ. The moment seen by the base of the part also increases with h, and this force can be many times larger as parts impact one another during assembly. While the restoring force increases as tilt increases they can only compensate for a limited amount of force which can easily be overcome as part the aspect ratio increases. For this reason it is easier to assemble parts with small aspect ratios.

www.manaraa.com

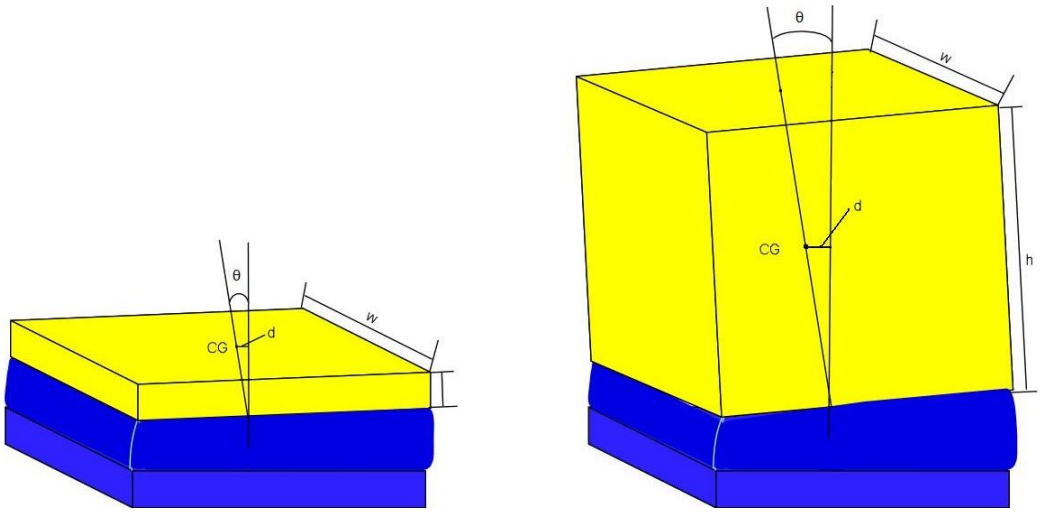

Figure 4: Illustration of different aspect ratio parts. Showing how the increase in height moves the center of gravity of the part further away from the aligned position.

2.2 Self-Assembly

The concept of self-assembly has been around since 1930. Self-assembly is first described in the theory of universal computation by Alan Turing in 1930[9]. It is mentioned in the theory of automata replication by John Von Neumann in 1950 and proven to exist by James D. Watson and Francis Crick in the discovery of the structure of DNA [9].

Following this seminal work, there have been several advances to self-assembly including research seeking to validate, optimize and achieve higher precision in man-made self-assembly processes. The following presents a

www.manaraa.com

general summary of these works and their contributions toward the assembly of thermoelectric coolers.

Though the idea of self-assembly has been present for a long time, it is not until recent years when Kazuo Hosokawa *et al.* demonstrated micro-scale self-assembly using surface tension in 1996 [9]. Since this early demonstration, there has been increasing interest in the use of self-assembly to assemble micro- and nano-scale structures which are costly, time consuming or impossible to produce by traditional methods of manufacturing.

The basis of self-assembly lies in templated self-assembly, where enzyme-mediated assembly occurs in nature to form needed tissues and cells of living matter. There have been many recent breakthroughs in showing the applications of self-assembly to micro- and nano-structures, that are too small to assemble using conventional means [4]. At very small size scales, gravity and inertial forces that are typically depended upon when performing assemblies, are not the dominant forces. Instead motion at the nanoscale is dominated by Van der Waals, electrostatic and surface tension forces. When scaling down in size, the pick-and-place assembly methods used on macro-scale parts to nano-scale parts face significant challenges when trying to overcome the lack of gravitational and inertial forces. [4, 10] This, combined with the fact that these methods cannot be performed in parallel assembly processes, has created a need to look for an alternate method of assembling thermoelectric coolers. Self assembly by definition covers any assembly of ordered components from a mixture of disordered components, without the manual or automated placement of

www.manaraa.com

components into their desired position. The only input to the system should be agitation of the components, which brings them in contact with the desired substrate locations; the agitation must be large enough to overcome local energy minimums so that the parts assemble into their positions at the predicted global energy minimum [4].

Several different energy potentials have been used to create self-assembly processes. These include magnetic, gravitational, electrostatic and interfacial potentials. [3, 11-14] All of these processes rely on the minimization of these potentials. These potentials can be compared to a ball resting on a hill, if some perturbing energy is supplied, the ball (self-assembly system) will eventually reach the global minimum energy so long as the perturbation is large enough to overcome local minima. There is also a limit to the maximum size of this input, if it is too large, it can overcome the attractive forces being used to assemble the system and release them from the site. This concept is illustrated in Figure 5.

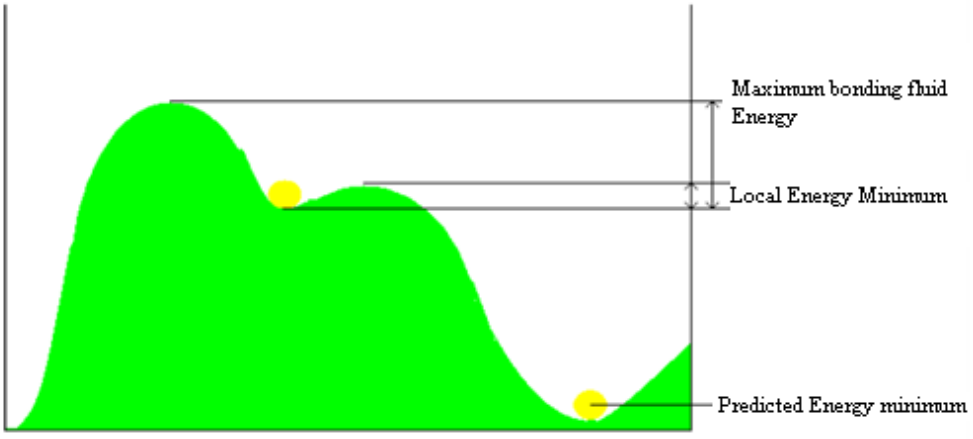

Figure 5: Ball on a hill analogy for system of potential energy.

www.manaraa.com

As stated there are several different forces that have been used in self-assembly work-to-date. As is the case with all self-assembly processes, the material properties of the assembled part put limitations on the methods of assembly. Several methods and their applications are described here; given the plethora of research in self-assembly a table summarizing these methods and their contribution to the self-assembly of TECs is given in Table 1 at the start of this chapter. A detailed review of the research which has been performed using each of the energies from the table is given in the following chapters.

2.2.1 Nanoscale Self-Assembly

While the assemblies being made are designed to work with microparts, there is also a large amount of work done on using self-assembly in the nanoscale. A brief summary of the major methods and characteristics unique to dealing with nano-assemblies is given as, ultimately, there could be nanostructure thermoelectric coolers fabricated through self-assembly [2].

Similarly to self-assembly in the microscale, nanoscale assemblies rely on setting up a system of carefully designed components and interactions so that the resulting formation forms structures based on the appropriate thermodynamic potentials such as Gibbs or Helmholtz free energies [15]. Many of the same forces that are used in nano-scale assembly will be examined further for the assembly of micro scale. These forces are Van der Waals, electrostatic, and magnetic forces [15]. There are some forces that are not strong enough for microscale assemblies, but do work in the nanoscale range such as molecular

www.manaraa.com

surface forces and entropic effects. The forces used in microscale assembly are described in the following sections.

Molecular surface forces refer to any one of a variety of short range attractive forces found at the molecular scale. These forces include covalent bonds, dipolar interactions, hydrogen bonding, and donor-acceptor interactions [15]. These forces have been used to create complex molecules, crystals and supramolecular architectures [16, 17]. These interactions have been used to produce ordered systems by coating the surface of nanoscale elements with various chemistries. Divalent elements in DNA assemble selectively and reversibly [18]. The use of dipole-dipole interactions between photoisomerizable surface groups enables rapid assembly and disassembly of ordered nanoparticle structures [15]. Entropic effects have also been used in nanoscale devices to complement dominant Van der Waals forces. One example is the use of molecular chains tethered to particles forming so called “brushes”[19]. This approach has long been used to stabilize colloidal particles. As can be seen from this brief overview of some of the research into nanoscale self-assembly there are a large array of possible assembly methods. While nanoscale self-assembly sometimes uses the same forces as microscale self-assembly, the processes will differ greatly due to the significant difference in size scale.

2.2.2 Electrostatic Forces for Self-Assembly

If the materials being assembled are capable of electrically charged, then this may be a possible method of assembly. Tien *et al.*[11] proposed a process of

www.manaraa.com

micro-fabrication by means of electrostatic assembly. This means of self-assembly has the potential to have fast assembly times due to the long range of the electrostatic interactions. The process was used in assembling 10 μm gold disks into disordered aggregates on charged surfaces. There were problems of overlapping pieces during assembly, which were reduced by making pieces with 1:1 aspect ratios [11]. The assembly was unlike many assemblies studied in that it was capable of orienting and placing two distinct sets of parts by taking advantage of both the attractive and repulsive forces present in electro static charges. Positively charged disks were deposited on phosphonate, carboxylate and SiOH-terminated surfaces. While negatively charged disks adhered to trimethylammonium and dimethylammonium-terminated surfaces [11]. This work shows promise of electrostatic self-assembly in systems where the particles being assembled are capable of holding a charge and are of a small enough size scale that the relatively weak electrostatic charges can overcome other forces. As such, electrostatic effects are more commonly used in nanoscale assembly.

Electrostatic forces have provided a basis for the formation of ionic, colloidal and macroparticle crystals. They have been used more recently in nanoscale assemblies to create diamond-like nanoparticle crystals, and to create robust monolayers and multilayer surface coatings [15]. Predominantly electrostatic forces are dominated by surface tension forces even in a non-liquid medium if the environment is not properly controlled. This is because moisture in the air creates a layer of water molecules on the surface of parts causing them to bond to other surfaces [20].

www.manaraa.com

2.2.3 Chemical Self-Assembly

While there are several papers which deal extensively with modifying surface properties of objects with chemical alteration, there are few methods which use chemical bonding as their sole means of attraction and bonding. One such process takes advantage of a phenomenon known as bridging flocculation. It is a colloidal phenomenon seen in the micro to millimeter size scale. Simply put the polymeric flocculent is added to a solvent where particles have been dispersed. By using the correct amounts of polymer and particles together in solution, the polymer will be absorbed into both particles bridging them together. Chemical assembly has some advantages in that the behavior of the self-assembly can be described by use of chemical formulae and analyzed by rate equations [13]. For work with assembling TEC elements it seems ill suited, as there is no obvious chemical polymer which will selectively bond our parts.

2.2.4 Van Der Waals Forces Used in Assembly

Assemblies relying on Van der Waals forces are using one of the most basic forces which dominate the micro and nanoscale ranges. Quite simply the bonding force here relies on the smoother surfaces of both part and substrate to hold parts in place after assembly in a fluidic medium. One of the earliest papers on self-assembly, Yeh *et al.* used fluidic self-assembly to place geometrically constrained parts into mated binding sites. The fluid was then allowed to evaporate relying on the Van der Waals force to hold them into place. An

www.manaraa.com

important aspect of the assembly to note is that it did produce working electrically connected arrays of GaAs LEDs, reporting a 90% success rate before evaporation. This is diminished to 30-70% after evaporation as many of the parts are pulled out of place by the receding liquid.

A similar process is examined by John Smith looking at a way to produce high density and low parasitic arrays of micro devices[20]. While the work gives few details there is a reported success rate of 99.99% for a process similar to that described by Yeh [20]. The parts are guided into place by use of hydrodynamic steering and oriented by precision micro machined substrates to match part geometries.

2.3 Capillary Self-Assembly

Surface tension forces are generally dominant in the micro and nano-scale ranges provided there is a liquid interface (in dry regimes electrostatic forces would be dominant). The surface tension force of the liquid on the binding site is the force which holds it to the site and controls the alignment of the assembled part. This surface tension determines the contact angle of the binding fluid.

www.manaraa.com

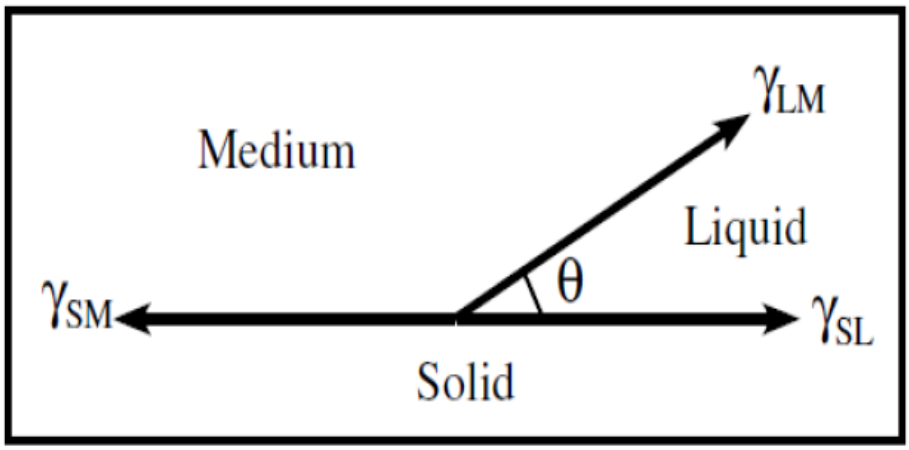

Figure 6: Contact angle caused by surface tension and the interface [21].

This relationship can be summarized in Figure 6 where γ_{SM} is the surface tension of the solid with the bonding medium, γ_{LM} is the surface tension of the assembly liquid and the bonding medium, γ_{SL} is the surface tension of the surface tension of the assembly liquid and the solid surface and Θ is the contact angle of the liquid [22].

These surface tension forces can even dominate gravitation forces in parts as large a $1mm^2$. Substantial surface energies are present at the interface between hydrophobic and hydrophilic materials [3, 23]. By controlling which areas are hydrophobic and those that are hydrophilic. This controlled combination of the interfaces between the assembly liquid and the hydrophobic and hydrophilic regions is the primary force for assembly. This force has been shown to be almost two orders of magnitude larger than gravitational forces by Greiner *et al.* [24]. A few of the needed concepts to understand the principles behind capillary self assemble are presented here. Several more examples of

www.manaraa.com

this process and relevant data are presented below. Manipulation and use of these interfacial forces is key to creating working assembly processes and several different strategies toward this end have been developed.

2.3.1 Self Assembled Mono Layers

Coincidently the same self assembled monolayer's (SAMs) developed through methods of nanoscale assembly prove themselves useful in manipulating the surface properties of parts and substrates during assemblies. The structure of the SAM molecules consists of a head group which is chosen based on the material of the substrate or part such that it will form a crystalline or semicrystalline structure. As mentioned previously this assembly is the result of nanoscale self-assembly and creates a single uniform layer on the surface. The tail is a hydrophobic group of molecules giving a uniform hydrophobic surface on the treated areas.

2.3.1.1 Analysis and Modeling

Böhringer et al. [25] performed an analysis on self-assembly by hydrophobic-hydrophilic surface patterning and capillary forces if an adhesive liquid between binding sites drives the assembly. These coatings are used to selectively coat regions of substrates rendering them hydrophobic. When these sites are passed through a layer of hydrophobic adhesive, they are coated. The adhesive performs three major functions in the assembly process; it acts as the local capillary force in binding parts, it serves as a lubricant to help ensure the

www.manaraa.com

absolute minimum energy state is obtained and finally it forms a permanent bond after the parts have been placed through capillary forces. Important data given in the paper includes the calculation of interfacial energies for SAM, water and hexadecane lubricant interfaces shown in Table 3. This is valuable information for assessing the viability of these interfacial energies in TEC assembly.

Table 3: Interfacial energies of SAM treatments.[25]

Interface	Interfacial Energy (mJ/m^2)
SAM-H_2O	~46
SAM-SiO_2	~46
SAM-Hexadecane	<1
H_2O- Hexadecane	52.2
H_2O- SiO_2	<1

2.3.1.2 Three-Dimensional Self-Assembly

While most of the research presented here is used to fabricate devices on a single plane at once, there has been some research into making three-dimensional structures using SAM treatments. Terfort *et al.* [26] used a combination of shape recognition and SAM treatment to several small self-assembled configurations. These included “doughnuts”, “footballs”, tetrahedrons and two part, capsule like structures. This work provides an interesting and

www.manaraa.com

unique use for capillary self-assembly, but other than common basic principles it offers little toward making a functional TEC.

2.3.1.3 Planar Assemblies

Most of the research done with capillary self-assembly falls into this category. While the term planar assembly might suggest a two dimensional assembly this is not always the case. Many times the assembly may be done on a device in a single plane with actuation or wafer to wafer transfer method used to create three dimensional devices.

Xiong *et al.* [27] presented a method of controlled multi-batch self-assembly of micro components using capillary forces. Arrays of gold binding sites were patterned using photolithography onto Silicon Dioxide wafers. Once these sites were exposed to an alkanethiol group SAM solution, they were rendered hydrophobic. The process used a hydrophobic adhesive to bind the parts in an assembly solution of de-ionized water. Without a SAM treatment the gold sites are inactive because the difference in surface energies is relatively small, as the sites are hydrophilic like the substrate. This very closely relates to what can hopefully be accomplished with the thermoelectric coolers. The desorption of SAMs through application of an electrochemical potential between the gold and the aqueous solution is also addressed. Using this procedure the sites were able to be selectively assembled by controlling activation and de-activation and thus obtained controlled multi-batch assembly of parts. The assembled LED arrays were permanently bonded on the substrate with the heat polymerizable adhesive,

www.manaraa.com

and the electrical connections to the substrate were facilitated with the electroplating of a tin-lead solder. While there has not been experimentation with SAMs for use in assembling TECs it has been examined and the information on SAM desorbtion provided here would be a necessary step to applying the process to make permanent electrical connections.

Singh B. P. *et al.* [28] presented a technique to assemble laser diodes using a guided fluidic assembly and reduce problems of improper orientation. As with many of the other processes this uses a shape directed assembly to help position the parts for assembly. The unassembled laser diodes are guided through a 150μm thick nickel mask into the recesses in the substrate. The parts are then secured into their final position using gravitational and capillary forces; this combination of the forces places the parts in a general location and then positions them with the capillary forces. Once the parts are assembled they are heat treated and then a performance characterization is performed. Different sizes of Laser Diodes are assembled successfully with a precision of 2μm and efficiency 100% assembly success. A flow chart detailing the automation capabilities of this guided fluidic self-assembly process are provided.

Fang *et al.* [29] proposed an assembly method using shape recognition with a capillary force interaction to drive the assembly. Several aspects of this assembly are unique and useful. These include high density assembly, process in open environment, peg free micro components, unique face orientation of parts, different modes of part mounting and unique face orientation of parts. The assembly of different types of components with similar dimensions and high

www.manaraa.com

surface coverage on the surface were achieved using the proposed technique. This was done by using 790 μm diced squares to complete the assemblies. A parallel assembly strategy is employed and the surface treatment of the diced parts is used to achieve assembly. Two different part shapes were used, those with flat edges and those with stepped edges. The assembly method includes plans for a vertical mode and a horizontal mode. The process is reported as having achieved 1000 densely packed parts in approximately 2 min and the defect rate is mentioned to be approximately 1%. With single batch presented result with surface coverage of 31% while a second run doubled this to 62%.

Scott *et al.* [30] proposed a parallel fabrication process to create micron-sized helical and toroidal inductors with Q values greater than or equal to 50 at multi-GHz frequencies. In order to increase the value of Q, the aspect ratio of the inductor must be as high as possible, because the Q value is directly proportional to the aspect ratio of the inductor. This self-assembly process allows multiple connections to a single inductor. Proper design of inductor was required so as to minimize the losses between the substrate and the conductor and increase Q value and operating range. The parts and substrate are both treated in the described process using hydrophobic parts and sites and a hydrophilic substrate. The work reports an assembly of an inductor with a Q value of approximately 60 at 5 GHz, with a resonant frequency of 9 GHz. The inductor shows a performance increase of three times that of a traditional lithographically fabricated inductor.

www.manaraa.com

Srinivasan *et al.* [3] demonstrated the self-assembly of parts with submicron positioning accuracy. The lateral alignment and the rotational misalignment are handled in the paper and a method of fluidic self-assembly is used. Different sized parts ranging from 150 x 150 x 15μm^3 to 400 x 400 x 50μm^3 were used in the assembly process. The parts were delivered and directed towards the substrate using a pipette. The accuracy of the assembly process is determined by the patterning of the hydrophobic shapes and the positioning depends on the resolution of these hydrophobic regions that are defined. A lubricant was applied to the hydrophobic sites to further increase their surface energy allowing a level of agitation which prevented binding of parts to each other as a result of the weaker capillary forces between them. The use of a quartz substrate was employed so that the accuracy can be determined by imaging the parts through the transparent substrate. The proposed assembly occurred in approximately 1 sec during the experimental verification of the proposed technique. The advantages of self-assembly over wafer to wafer transfer were given, reporting a maximum precision of 0.2μm and a rotational misalignment of approximately 0.3° were reported. The work reports a rate of one 98 part array in 1 minute with 100% of the available sites binding to parts, and proper alignment on all sites.

Srinivasan *et al.* [23] also proposed a similar method of fluidic self-assembly technique using capillary forces to assemble micro parts with high alignment precision. This time to make the assemblies more permanent, a heat curable acrylate adhesive was used to provide capillary forces and was

www.manaraa.com

polymerized in a bath of water at 80°C for 16 hours with continuous nitrogen bubbling to secure the parts. The fill factors were measured to be 95% and the assemblies were measured to be free of tilt to within 6nm rms. Further investigations of the process are given including reducing the mass of the assembly parts, characterizing the adhesives and proper tune of bind site area to produce different levels of adhesion. This process is a promising method of assembly, but would require far longer than a solder based assembly to complete a batch due to the lengthy curing process of the curable acrylate.

2.3.2 Using Solder as an Assembly Medium

Several different researchers have done work with self-assembly using a variety of different methods and materials to test the theories of self-assembly and make numerous devices. Many of these researchers have performed tasks similar to those needed to assemble the thermo electric coolers and done other pertinent research into the behavior of these low melting alloys and their applications to capillary self-assembly.

Green *et al.* [31] claims to have developed the first self assembled three-dimensional microstructures by using solder surface tension to produce out of plane motion. They fabricated an array of nickel and copper regions on Silicon substrates and using an electroplated solder pad. The solder was heated to allow reflow lifting one of the arrays approximately 90 degrees out of the plane. This early work has been expanded on by many researches and the actuation of microscale hinges through solder reflow to refine accuracy and yields are the

www.manaraa.com

topics of many papers which will be discussed in detail later. There have been many interesting and functional solder based assemblies created to date as well.

2.3.2.1 Functional Assemblies

In the past decade or so several researchers have produced in and out of plane self-assembled structures through use of solders capillary forces. Zheng *et al.* [10] proposed the use of low temperature melting point alloys for assembly of functional LED micro components having three dimensional structures. The structure contains an LED component, an encapsulation body with solder bumps to act as binding sites and a chip carrier. The proposed method of assembly involves the use of capillary forces of the low melting alloy to drive the assembly. This method combined the shape recognition and solder directed method of self-assembly together in order to accomplish a multi-part and multi dimensional assembly. While this method explored the option of assembling heterogeneous micro systems, in three dimensional space, the process used a sequential feed technique to assemble the elements sequentially and not in parallel. The paper reports on few good techniques for increasing yield such as tighter packing of binding sites and the used of four-fold symmetry over a two-fold symmetry attempted easier.

Cannon *et al.* [32] proposed a method for the self-assembly of millimeter scale parts into 5 mm cubes of polymethylmethacrylate. This work deals with the local and the global energy minima in assembly. It shows how the capillary forces serve as the driving force behind self alignment. The research reports the self

www.manaraa.com

assemblies of parts with a variety of functions being assembled in to three-dimensional structures, enabled by creating a standardized interface for the parts. The process reported an assembly rate of 0.125 components per second with a 93% yield rate. Process modifications including using density stratified solution or molding alignment features so as to accept or reject parts by design have also been addressed in the paper. A novel aspect of the method is that the polymethylmethacrylate can form an encapsulation for any number of different devices and assembled them into a three-dimensional network. Though this method is designed currently to handle parts of 5mm it could possibly be adapted to smaller elements, though it would require an alternative way to manufacture the assembly structure.

Smaller three-dimensional circuits using self-assembly have been accomplished by Gracias *et al.* [33]. The process consists of stages of series and parallel connections, to make the electrical networks. To complete this network LEDs were mounted onto faces of truncated octahedrons. The part sizes used in this work had 3mm faces with ~ 1mm solder dots to bond the parts. The work produced functional parallel and series electrical connections to the three-dimensional network. It is important to note that the research also indicated that so long as the wire pathways were kept small (~150 μm) the solder film deposited on them would be significantly smaller than that of the contact pads(~15% of the total height). This fact is important for simplifying the assembly of TECs because it means there should be little concern of the electrical

www.manaraa.com

pathways interfering with our contact pads so long as their width is kept significantly smaller.

Some structures have been fabricated with solder based self-assembly in planer substrates as well. Schuylenbergh *et al.* [34] produced high quality inductors by self assembling pieces of stressed metal onto substrates. The metal is then wet etched to release the stress in the top layer curling it into a coil for the inductor.

Jacobs *et al.* [35] has also produced a notable device by attaching LEDs to a flexible substrate. The self-assembly of these elements was accomplished using low melting point solder and patterned copper binding sites. The LED orientation was determined by the size of the contact at each end, only the side with the larger contact would have the surface tension required to stay bonded with agitation of the system. The work reported successful assemblies with some errors. The errors encountered included parts bridging two sites, parts attaching themselves to solder on wire connections and two parts occupying the same. Still they reported 98% coverage in 3 minutes on a 1600 site array. The work provides several important observations toward the assembly of TECs. It is the closest physical assembly this literature search has produced in that it relies entirely on solder to attach and locate the parts as well as binding them. The research uses the same compound of low melting alloy used in our TEC assemblies.

www.manaraa.com

2.3.2.2 Lubrication

To assist in the orientation of solder assemblies many researchers have used lubricants. The advantage of lubricants is to help parts overcome the challenge of fine alignment on the binding sites. As mentioned early the restoring forces seen by parts are significantly diminished in this region and will often not reach exact equilibrium because of this. Scott et al. produced high-performance inductors using such a method. The method involves making a hydrophobic region around the binding site which will attract the lubricant, in this case hexadecane, to cover the binding site. So long as the hexadecane is pure there should be no problems forming an electrical connections when the solder is reflowed [30].

2.3.2.3 Bonding Fluid Volume

Excess bonding fluid on the binding site can permit horizontal displacement off the pad or unwanted tilt in the parts. Controlling the volume of the bonding fluid applied to the binding site is an important step in creating a successful assembly process [24]. Finding the appropriate fluid volumes and developing a method to reliably deposit the correct volume is a primary concern of this research.

www.manaraa.com

2.3.2.4 Geometric Constraints

Many major advances in the use of geometric constraint have proven their usefulness in creating both three-dimensional and planer assemblies by aiding capillary forces in precision alignment. The first of these is a work by Zheng *et al*. [36] who made three dimensional LED encapsulations using Pyrex pieces with four-fold symmetry. Using the capillary force of solder the parts were bound together and electrical connections were made. Geometric constraints in planer capillary assemblies were performed by Jacobs *et al.* [37]. Using structures which confined 3 degrees of freedom once the parts were affixed to the solder resulted in accuracy of 0.3° and contact pad registration with an accuracy of 19 μm. These geometric constraints offer a possible solution to slight misalignments sometimes seen in the assembly of TECs.

2.3.2.5 Modeling Solder Assemblies

Two major works have contributed to the modeling of solder surface interactions for use in assembly. Both papers make use of a program named Surface Evolver which uses finite elements analysis to analyze forces present in fluid droplets. The program is capable of calculating the magnitude and directions of the capillary forces seen during assembly and finding the equilibrium position of the part on the droplet. Valuable contributions from each work are expanded upon below.

www.manaraa.com

The first of these is work done by Stauth *et al.* [38] detailing the forces seen by silicon components attempting to assemble in the presence of a fluid flow. The work provides relevant data by finding the surface tension of the low melting point solder to be 400 dynes/cm as measured by contact angle. The paper goes on to give a graphical representation of the relationship between part displacement and capillary for a small 10 x 50 x 300 μm^3 silicon part. The model works over a range of displacement between 0 to 12 μm. The force was small and varied between 2 and 2.5 *n*N. The model clearly shows that the part will find its minimum energy when it is centered on the pad.

The second of these works modeling surface energies was performed by Greiner et al. [24]using a lubricant as a bonding fluid. Models created here predict not only the shift displacements of the part, but also tilt, twist and lift. It is shown that lift and height follow a fairly linear curve with rather large restoring forces until the parts is in equilibrium. The paper does mention that excess amounts of bonding fluid can create unstable configurations and the restoring force is greater when there is a small volume of bonding fluid. By far the most important aspect of this paper is it analysis of shift and torque on parts which was found to be harder to control when compared to tilt and lift. This is important because it shows why obtaining parts which are close to correct in orientation, but not exact can happen easily.

www.manaraa.com

2.3.2.6 Self-Folding Solder Hinges

As was mentioned previously since Greens initial out of plane assembly of a solder hinge several other researchers have worked with using solder to actuate hinges improving on technique and accuracy. Theoretical work on using solder actuation for the rotation was theoretically developed by Syms [39] in the early 90's. In this work a number of equations were developed and simple mathematical models were carried out to show that the volume and surface tension of solder could be used to predict the rotation of parts and optimal solder volumes could be found from the data. The paper also went on to calculate the torque seen by the rotated part at different angles of rotation.

As previously stated Green and Syms developed the first three-dimensional micro structure not long after this initial theoretical work was published. The structures were simple grid shaped arrays of etched Silicon and Nickel. While the device proved the functionality of the theory it did nothing to further the development of the model, because no accuracy measurement was performed. Though in a publication shortly after this Syms refined the model by incorporating a balance of the surface energy in place of the torque balances used in the previous work. By doing this he clearly showed how the surface tension force provided by the solder is dominant over other forces in this size range. Important to future work in this field, the paper also established a precedent that a physical hinge for the parts was unnecessary so long as the parameters were appropriately controlled [40]. Syms would later go on to produce rotational self-assembly of complex microstructures by using

www.manaraa.com

borophosphosilicate glass as the meltable material. The process overcame many of the problems experienced by works using solder, producing greater control of angular orientation. This was primarily due to the less dramatic change in viscosity experienced by the glass when compared to solder. The glass was also superior in that it did not experience problems with oxidation and corrosion that solder had.

Around this same time Lin *et al.* [41] produced detailed modeling of solder joints to show the relationship between solder volume and restoring force. It was shown that smaller volumes of solder produced slightly larger restoring forces, a finding which concurs with the findings produced by Syms. The model goes on to take several sets of data and fit them to a polynomial regression to create a fit for the relationship between surface tension forces and solder joint design. Similar to Lin et al. Bingzhi et al. produced a work which studied the forces created on assemblies by solder connections. The work considered parts of varying lengths being subjected to external flows. In addition, the research also varies the flow rate and solder height and relates them to part displacement. The results indicated that the flow effects could be neglected so long as the part size was under 5 x 5 mm^2 [42].

Another use of these capillary forces for use in precision alignment is used to place computational chips. Jairazbhoy [43] presented an analytical prediction of the shape and solder heights of equilibrium joints formed due to the solder re-flow in surface mount components. This is a common process used in the manufacture of printed circuit boards. The analysis considers two dimensional

www.manaraa.com

joints with negligible solder density effects. Simple experimental results were done to validate the calculations. A numeric analysis of the solder joint geometries as well as physical properties was also performed. Small changes in these properties have larger potential heights at constant solder volume and reliability of the solder joints is closely tied to these basic properties. The information provided here is very useful in predicting the shape of the solder and the standoff heights when considering solder-based assembly. Still while analysis predicted the perfect assembly of predictable solder joints the development of physical devices lagged behind.

For almost a decade after Syms had predicted the alignment of solder joins to precise amounts, experimental results had at best yielded ±2°. It was not until Harsh et al. designed an in plane locking mechanisms that solder hinges saw ±0.3° of misalignment [44]. The process was designed to be batch compatible so that hundreds or thousands of parts at a time can be assembled in a single reflow process.

The solder hinge has also been applied to actuate a micromirror device. Mcarthy *et al.* [45] describe a method of fabrication and actuation of a micromirror. The device was capable of stable rotation ±10° from the assembled position under the application of a 200V actuation voltage. The design incorporated the surface tension of the solder with several geometric constraints to achieve the desired result. Much like these later hinge assemblies many making planar assemblies have found geometric constraints to be a useful tool in increasing assembly accuracy.

www.manaraa.com

2.3.3 Magnetic Assisted Assembly

Another possible driver of self-assembly, to be considered, is magnetic force. This process uses the natural tendency of opposite magnetic poles to attract. By creating a system of the appropriate magnetic fields, the assembly yield and accuracy can be significantly improved. There are several drawbacks to this method. The foremost of them being that the parts must have a magnetic component in order to be able to be assembled with this method.

Techniques of assembly involving magnetic forces to aid in assembly are given by Shet *et al.* [46]. Two techniques are presented, one for in plane parts in a batch assembly and another for a feed tape technique. The most useful to examine for work with TECs, is the in plane assembly technique. This work shows that the process has some advantage in being able to be performed in a clean and dry assembly environment, in contrast to the capillary assembly method being proposed, which requires the assembly to be in some form of liquid. The process involves the creation of a magnetic guide layer on the top layer of the wafer, by coating it with a magnetic material and supplying it with a magnetic field. A permanent magnet rotated near the system is used to provide agitation of the parts. The advantage to this technique is that the nanodevices being placed are always placed in the correct orientation bases on the location of either cobalt or nickel plating. The technique has not been validated experimentally from the research found to date.

Some of the most simple are the assembly of magnetic micro and nano particles into arrays. Assembly of Nickel nano particles has been accomplished

www.manaraa.com

by Srikanth [12]. The nano particles were arranged into nanochains using the presence of a 250 Gauss magnetic field. Similarly, research has also made use of magnetic forces to create functional micro devices. Choi et al. has used magnetic fields to assemble arrays of Au, Ti and Ni into a functional biosensor. The analysis of the assembly did not detail accuracy, but the reported success rate was 71%. The nickel Layer was used to control the placement of the arrays which were composed of a 1:1:2 ratio of Ti, Au and Ni [47].

On the larger scale Shetye *et al.* [48] proposed a method of magnetic assembly capable of orienting and placing 1 mm x 1mm x 0.5mm Silicon parts onto a substrate. The process used magnets bonded to the Silicon parts and substrates. By creating recesses in silicon wafers, a magnetic powder was filled in and locked into place using a wax. The research examined several different situations including part to part bonding and part to substrate bonding.

While magnetism certainly has some advantages, in that is has both attractive and repulsive forces, it can be performed in a dry environment and it can have relatively large force ratios when compared with other assembly methods. However, without having parts which can be easily magnetized, the method is ineffective. Assemblies to date, show that magnetic assembly can be used effectively to influence very small particles of ferromagnetic material so long as the ratio of ferromagnetic material to non magnetic material is sufficient. In order to influence larger parts the use of permanent magnets on the parts had to be used. This research suggests that magnetic assisted assembly would likely

www.manaraa.com

only be an option with thermoelectric elements, but certainly not a viable tool for assembly of our parts on the microscale.

www.manaraa.com

Chapter 3 - Experimental Methods

The methods used in the self-assembly of TECs are presented here. The methods of fabrication and the materials used are described first. This is followed by a section briefly describing the challenges in selecting these materials. Next, a detailed outline of the assembly process is given, followed by its application in experimental assembly of the TECs. Finally, a method for trying to improve the assemblies by more accurately controlling solder deposition on the sites is explored.

3.1 Fabrication Methods

There were multiple methods used to fabricate substrates and assemble devices. These methods were largely dictated by the size of the devices being assembled and the materials available. These methods include the use of CNC milling at larger size ranges and photolithography for smaller features.

3.1.1 Laminate Substrates

The first thermoelectric elements assembled were .055”x.055”x.067”, giving them an aspect ratio of 1:1.22(length: height). Because the dimensions of these parts were large enough to be fabricated on a CNC mill, one was used. The process started by applying copper tape to an electrically nonconductive

www.manaraa.com

laminate substrate .010” in thickness. A .003” engraving tip was used in the CNC mill to trace out the assembly sites and cooler circuit. Once the pattern was milled, the surface was gently abraded to remove excess material from milling and remove corrosion from the surface of the tape. The excess tape was then removed leaving the assembly sites and circuit patterns behind on the laminate. The sites fabricated can be seen in Figure 7.

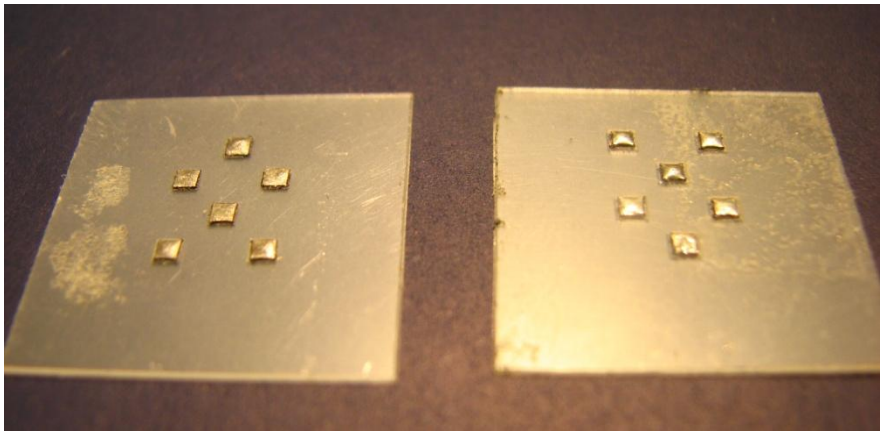

Figure 7: Substrates made by patterning copper tape using a CNC mill.

3.1.2 Silicon Substrates

For the next size of thermoelectric elements, the dimensions .025”x.025”x.025” (an aspect ratio of 1:1) were used. This size range could not be fabricated using the CNC mill, largely due to the limitations of the adhesion of the copper tape. Instead photolithography was used on silicon wafer substrates. The process started with bare silicon wafers, on which 5 kÅ of oxide was grown to act as a electrically insulating layer. The wafers were then cleaned using

www.manaraa.com

acetone and methanol and rinsed with isopropyl alcohol. An adhesion promoter (HMDS) and Shipley 1813 photoresist were spun onto the wafer at 2200 RPM. A mask was printed on 7 mil Kodak photoplotter film APR7 with light features. The resist was then exposed using UV light and allowed to develop in Shipley MF-319.

Once the photoresist was patterned, an electron beam evaporator was used for metal deposition onto the wafers. First, a layer of chromium is deposited to a thickness of 200 Å to promote adhesion of copper and gold coatings. Secondly a layer of copper or gold is deposited on top of the chromium to a thickness of 1kÅ.

The wafers are then soaked in acetone to dissolve the remaining photoresist taking with the unwanted metals with it. This liftoff process leaves only the assembly sites and electrical circuits remaining on the wafer. The wafers are coated with another layer of Shipley 1813 to protect them from corrosion and oxidation during cutting and storage. Finally, they are then diced into .325”x.525” rectangles. The parts are then coated with their appropriate alloys. The temporary substrates use the lowest melting point solder. The fabricated substrates can be seen in Figure 8.

www.manaraa.com

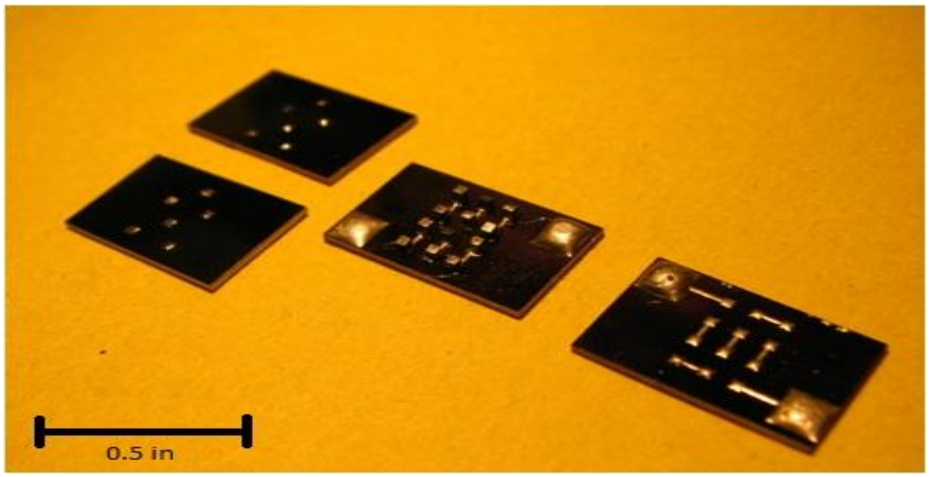

Figure 8: Diced silicon substrates made using photolithography and e-beam deposition. Coated with low melting point alloys.

Coating of solder on the parts was accomplished by heating a bath of solder on a hot plate. A solution of slightly acidic DI water and sulfuric acid was used to prevent oxidation of the solder, the same solution used in the assembly trials. It was noticed that many times, especially on smaller site sizes, the solder did not wet thoroughly to the substrates. In this situation, application of ultrasonic vibration from a sonicator was used to aid in the deposition. Several short bursts of sonication provided vastly improved wetting on these difficult to coat sites.

3.2 Basic Assembly Steps

Assembly of the thermoelectric elements is theoretically possible, as demonstrated by other assemblies that have used low melting alloys [49]. There are however many obstacles that need to be overcome to make the process

www.manaraa.com

successful and repeatable. These include selecting proper materials, developing an assembly process and preparing the substrates for the assembly.

3.2.1 Materials

There are several materials involved in the assembly process. The first step is to find a suitable assembly fluid; for many low melting alloys de-ionized water is an acceptable solution. However, if the bonding medium requires a temperature at or above 212°F, ethylene glycol can be used as an assembly fluid. In order to combat the constant oxidation experienced by the low melting alloy while heating an acid must be added to the assembly fluid to render it slightly acidic. Testing was performed on a sample of solder, copper, and thermoelectric elements to attain an idea of their susceptibility to corrosion due to extended exposure to acidic solutions. It was found that a pH of 2-2.5 provided adequate removal of oxides from the solder while allowing enough time to make the assemblies without irreparable damage to the substrates or parts, as shown in Figure 9 where samples were exposed to a 2.0 pH solution at 165 °F for 10 minutes.

www.manaraa.com

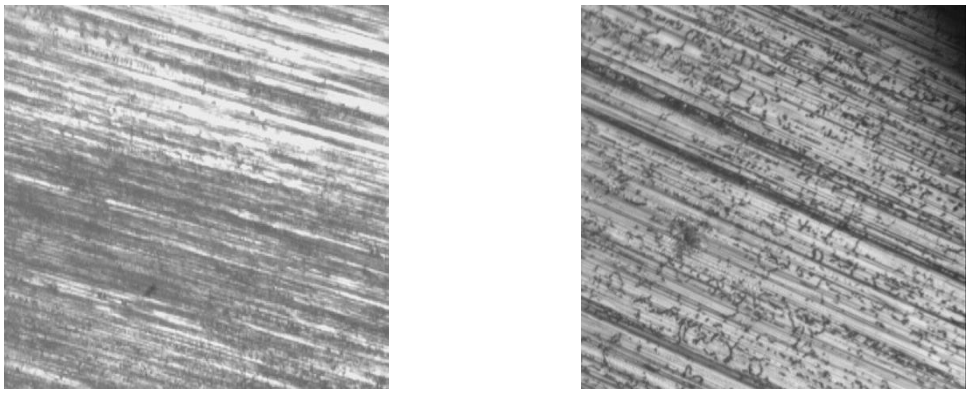

(a) (b)

Figure 9: Images showing the corrosion experienced by copper. Pictures (a) and (b) are pictures of copper tape, taken at 10x under an optical microscope, before and after being exposed to a 2.0 pH sulfuric acid solution for 10 minutes at 165 °F. You can notice small defects going against the grain of the copper from the corrosion in b.

Finding a suitable bonding fluid is also imperative for proper assembly. Low melting eutectic alloys of bismuth, lead, tin, cadmium and sometimes indium, have been previously used to create assemblies [33, 49]. Two compounds in particular were chosen, having melting points of 117°F and 158°F, because both can be used with water as an assembly fluid. A number of problems in wetting resulted from trying to reuse these solders, likely due to their separation and deterioration during heating and cooling while being exposed to an acidic solution, for this reason fresh solder should always used during assembly.

www.manaraa.com

3.2.2 Process

The process suggested by Crane *et al.* [6] for assembling the thermoelectric coolers involves several steps. The first step is to place the parts to be assembled onto specially designed sites. Once assembled, the parts will be transferred onto a circuit in order to make a thermoelectric cooler. In order to transfer the parts successfully, one of the pair of bonds must be significantly stronger than the other. In our assemblies, this was done by using two separate temperature solders so one would be solidified during the transfer. In order to easily remove the temporary substrate, the higher temperature solder is placed on the final substrate.

3.2.3 Substrate Preparation

Application of solder to the substrates is accomplished by dipping them through the slightly acidic solution into the molten solder. For the smaller feature sizes it was often difficult to get the solder to wet completely. It was found the addition of ultrasonic vibration greatly improved the application of the solder in these situations. The vibration had to be applied in short bursts, or it could prove too strong, actually removing solder from the sites. The temporary substrate was coated with the lowest melting-point (117°F) alloy. The final substrate refers to substrate containing the electrical circuit to which the thermoelectric parts must be attached in order to form a thermoelectric cooler. This piece it is coated with the 70°C melting point alloy.

www.manaraa.com

3.3 Assembly of 0.055” Element Cooler

The assembly process while simple in theory presented some problems in practice. First, finding a suitable container in which to perform the assemblies, can prove challenging; bottles with any sort of gaps around the lid or cover were prone to trapping most or all of the parts in these crevices, especially when dealing with smaller part sizes, for this reason the process was changed slightly between the 0.055” and 0.025” part sizes.

The 0.055” parts were assembled in a cleaned plastic container with flat sides. Using double sided adhesive tape the assembly substrate was attached to the container. Another layer of tape was also placed on top of the substrate, as shown in Figure 10. The bottle was then filled with a mixture of DI water and sulfuric acid with a pH of 2.5. A hot water bath was used to hold the parts at 55°C while the container was rotated, after 10 minutes of this agitation, the container was opened and the assembly checked.

www.manaraa.com

Figure 10: Laminate substrate constrained in the small plastic container before an assembly test.

Using this method, some successful assemblies were made. However, the completely random interactions of the parts within the much larger volume of the container led to long assembly times. Many times this caused irreparable damage to parts and substrates, in the form of corrosion previously discussed, leaving unfilled bonding sites. The key to resolving this issue was ensuring that the pH of the assembly solution was kept only as acidic as was needed for the assembly. Additionally, the assembly should be completed in as short a time as possible; the parts removed and rinsed immediately following their assembly. In the later smaller assemblies a new method of part agitation was used to further reduce assembly time.

www.manaraa.com

The successful assemblies were used in the transfer process to create a thermoelectric cooler. The transfer process started by creating a holder that ensured alignment of both substrates by geometrically constraining them. The substrates were then placed into the holder face-to-face with the final substrate on the bottom and locked in place. The holder and substrates were then immersed in slightly acidic water at 75°C while a slight pressure was applied to the top substrate to ensure the parts contacted the solder on the final substrate. This position was maintained for 1 minute. It was noticed that a slightly stronger acidic solution was helpful in this step (~2.0 pH). This ensured that there was no oxide on the contact pads and the period of exposure to the acidic solution during this phase was limited enough that significant damage to the parts and substrates was not noticed.

Once it was observed that the parts were bonded to the final substrate, the entire assembly was taken out and rinsed gently with DI water solidifying all the bonds. A second beaker of water was heated to 55°C, allowing the lower melting point solder to become molten while the other stayed solid. The temporary substrate is then easily removed from the final substrate, because the higher melting-point solder was still solid. The process was then repeated again with the thermoelectric elements of opposite doping. Once *n* and *p* type elements were together on the final substrate, another bath of slightly acidic water was heated to 75°C and the assembly transfer process was repeated. At this stage, in place of a temporary and final substrate, the mated pair of final substrates were used. Once the parts were bonded to both final substrates the assembly was

www.manaraa.com

once again rinsed and the assembly was complete. Different stages of the assembly are shown in Figure 11. The assembly was checked successfully for conductivity; however, assessment of its thermoelectric properties was not performed.

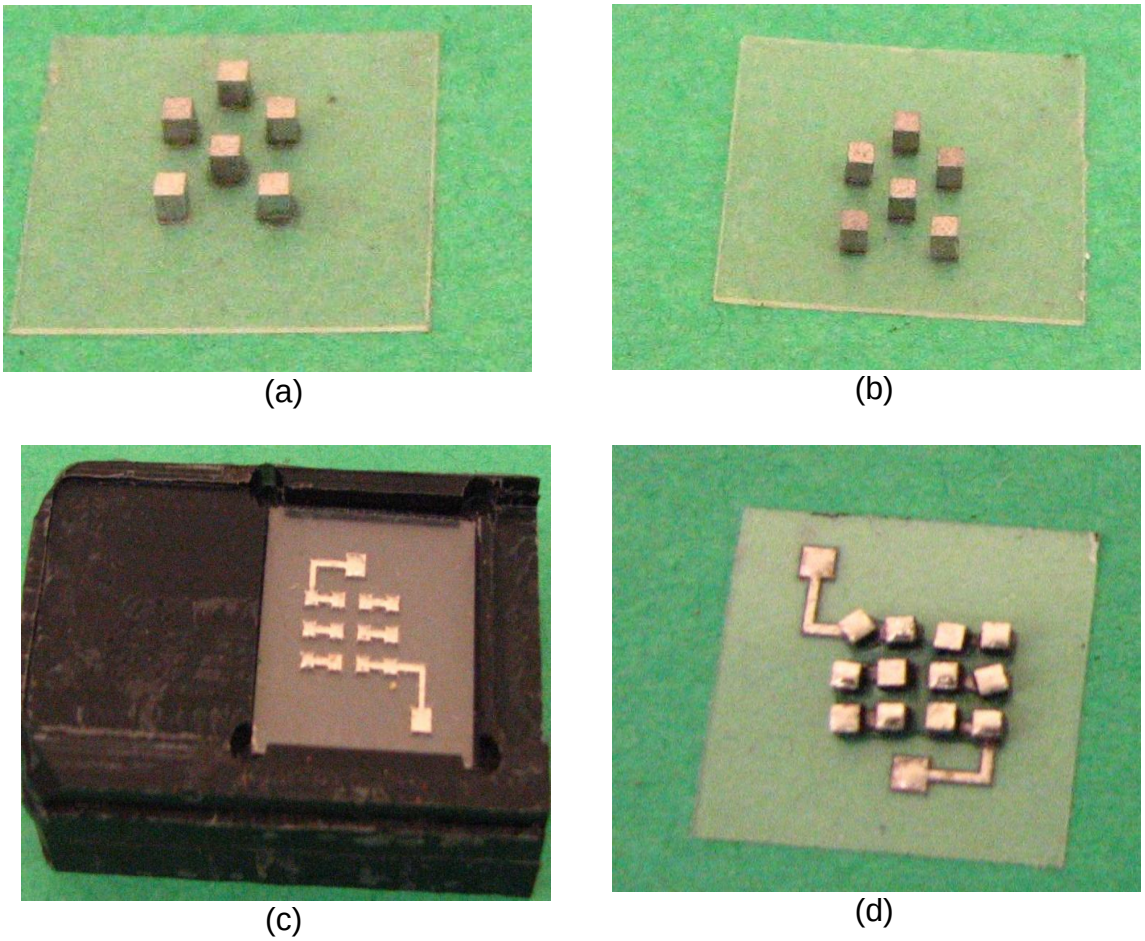

Figure 11: Pictures outlining key stages in the assembly of 0.055" bismuth telluride elements. Pictures A and B show the elements which have been self assembled onto temporary substrates. The elements are then loaded into the holder pictured in C in 2 separate transfer processes. This creates an assembly of both types of elements as pictured in figure D.

Another issue which arose during the assembly of this TEC was the misalignment of the transferred parts. This can be seen clearly in several of the

www.manaraa.com

elements in the TEC assembly pictures in Figure 11d. As was found by several researchers the parts are less likely to align when they are stuck in local minimums of energy near the desired alignment location. While this is not currently causing the assemblies to fail it is a problem which will need to be addressed in order to more closely pack the elements in future assemblies.

3.4 Assembly of 0.025" Element Cooler

The assembly of the smaller 0.025" parts was performed in a similar manner. However, some of the processes were changed to accommodate the smaller size scale. The closed container and hot water bath were replaced by a 150 ml beaker and a hot plate. The same 2.5 pH deionized water and sulfuric acid solution were used. The open beaker allowed for the parts to be manually agitated by use of a pipette. To accomplish the agitation, a large number of parts were repeatedly picked up and expelled near the substrate. After approximately five minutes of this agitation all sites were assembled. The process was performed on both *n* and *p* type elements. A new substrate holder had to be fabricated for the smaller sizes. However, the transfer was performed in almost the same manner. The primary difference in the transfer process was the addition of fluid flow into the transfer holder, the addition of a channel for fluid injection can be seen in Figure 12(c) in the upper right corner of the substrate holder. This ensured that fluid reached all the elements in the transfer process to both remove oxides and heat the solder to the melting point.

www.manaraa.com

Unlike the design for the 0.055” parts, the 0.025” final substrates had a pair of larger contacts which served two purposes. First, they provided an area large enough to solder a wire connection by hand. Secondly, they provided mechanical support for the device where the solder contacted both of the final substrates with a greater surface area than that provided by the elements themselves. The results and materials used in this process are shown in Figure 12.

www.manaraa.com

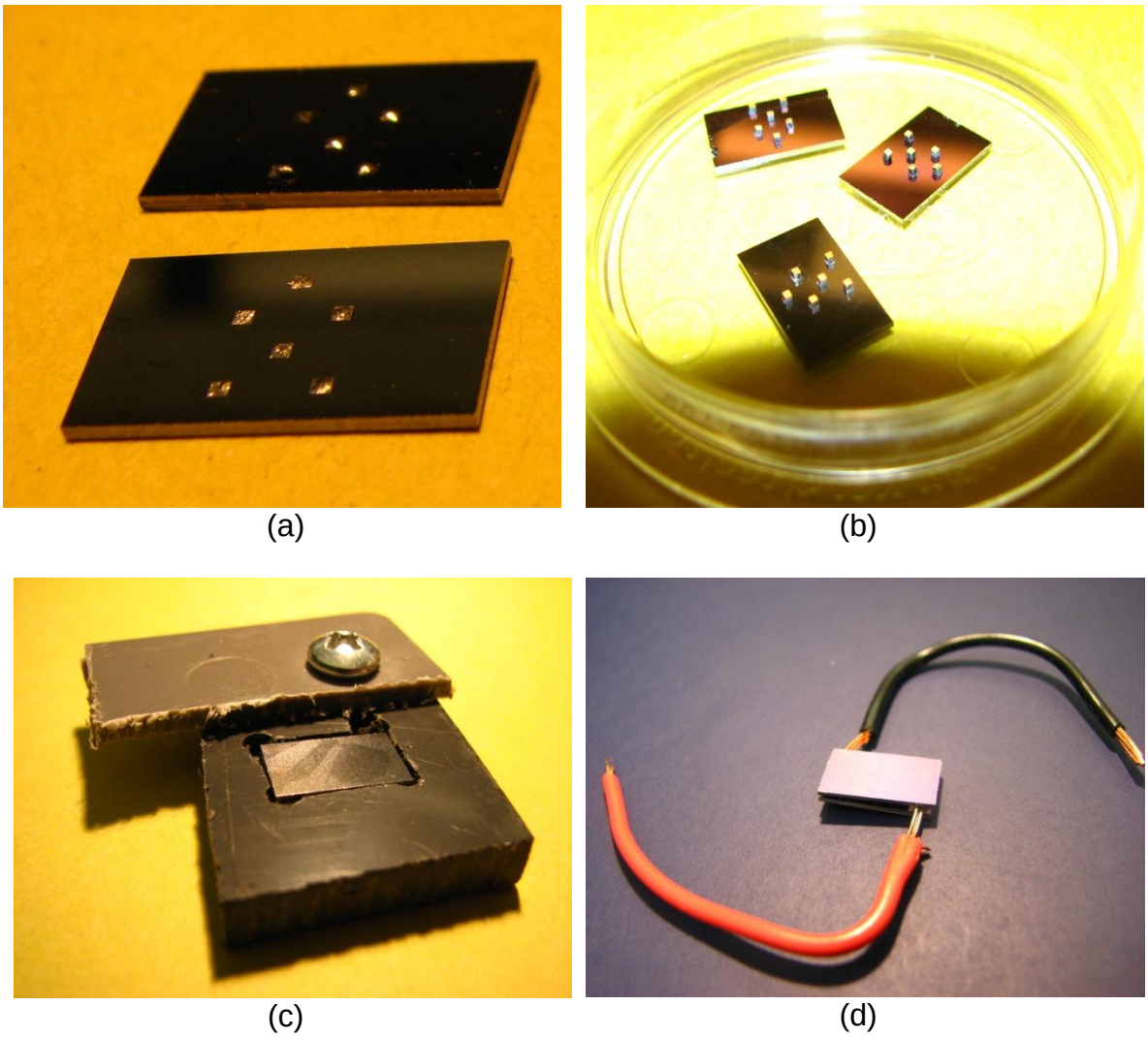

Figure 12: Pictures showing the process of assembling 0.025” bismuth telluride elements. The transfer substrates are shown in (a). The thermoelectric elements are then assembled to them in (b) and transferred using the holder pictured in (c). Then a top substrate is added and the final cooler if shown in (d).

3.5 Centrifuge Design

A device to centrifuge parts was created for several reasons. The first of these was to create an environment where parts resting on molten solder could be tested under different amounts of acceleration to assess the forces they could

www.manaraa.com

withstand before separation. In order to accomplish this, the parts would be recorded while experiencing acceleration in the centrifuge to view their displacement. This testing could be used to validate the surface evolver models developed by Stauth and Greiner [24, 38].

Another function of the centrifuge was to apply a force to the solder on the assembly sites, removing the excess. Early on in the assembly trials it was noticed that problems with initial assembly and transfer resulted from some of the sites being coated with excess amounts of solder. This problem often resulted in parts being far out of alignment. In some cases excess amounts of solder even lead to multiple parts bonding onto the same site, as shown in Figure 13.

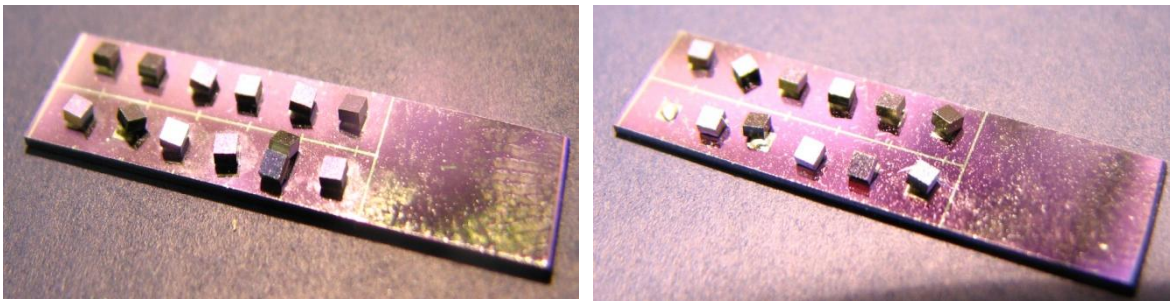

(a) (b)

Figure 13: Picture (a) and (b) show early assembly trials using Si parts. In (a) there is a site with 2 parts bonded to it as well as parts experiencing significant misalignment. Picture (b) shows a site missing a part and also several parts out of alignment.

The centrifuge was turned using a 120V AC, ½ HP, 10,000 RPM electric motor. The arm is made from a 16”x4” bar of aluminum stock. Two pockets were milled into each end of the bar. A stepped design was used to allow several parts to be tested at once in both horizontal and vertical positions. The bar is supported by a 5/8” aluminum shaft, turned down at one end to prevent the bar

www.manaraa.com

from sliding down and held in place with a locking set screw. A 3 point self centering chuck was used to hold the bar in place. A plate was fabricated to hold the chuck and motor in place. Two pulleys and a notched v-belt were used to reduce the speed and increase the torque seen by the arm by a 5:1 ratio. The plate is mounted to a framework of 80/20 extruded aluminum bars to provide a stiff support. Basic calculations were done to assess the amount of support needed. A simple 1 x ¼" steel beam was used to calculate the natural frequency of the system. First a spring constant k had to be established. Through the use of beam tables we were able to calculate a deflection based on a model of a simply supported beam with a concentrated loading in the center to find the maximum possible deflection[50],

$$y_{\max} = \frac{F}{3EI}\left(2a^3 - \frac{a^4}{l} - la^2\right) \quad (7).$$

Once the maximum deflection was found the natural frequency was easily calculated by estimating the mass of the system at 30 lbs and using the formula,

$$\omega_n = \sqrt{\frac{k}{m}} \quad (8).$$

Using these calculations the natural frequency was found to be around 20 Hz, this was lower than would be optimal for our testing so a stiffer support was needed. As adding thicker or wider steel beams would be only slightly more effective and increase the weight of the system significantly. Instead using Aluminum 80/20 beams, whose geometry was much more suited for resisting

www.manaraa.com

deflection was chosen, giving the additional benefit of assembly with minimal machining as well.

The entire framework was placed inside a wooden box to provide a base and contain the parts in case of unforeseen failure. An adjustable speed controller and emergency shutoff are then attached to the outside cover, and an acrylic window is hinged to allow visual inspection of the centrifuge during operation. The enclosure for the centrifuge can be seen in Figure 14 and a detailed picture of the components in Figure 15. CAD models of the arm showing its design features and testing locations can be seen in Figure 16 and Figure 17 respectively.

Figure 14: Centrifuge assembly with clear window, speed controller and emergency stop button.

www.manaraa.com

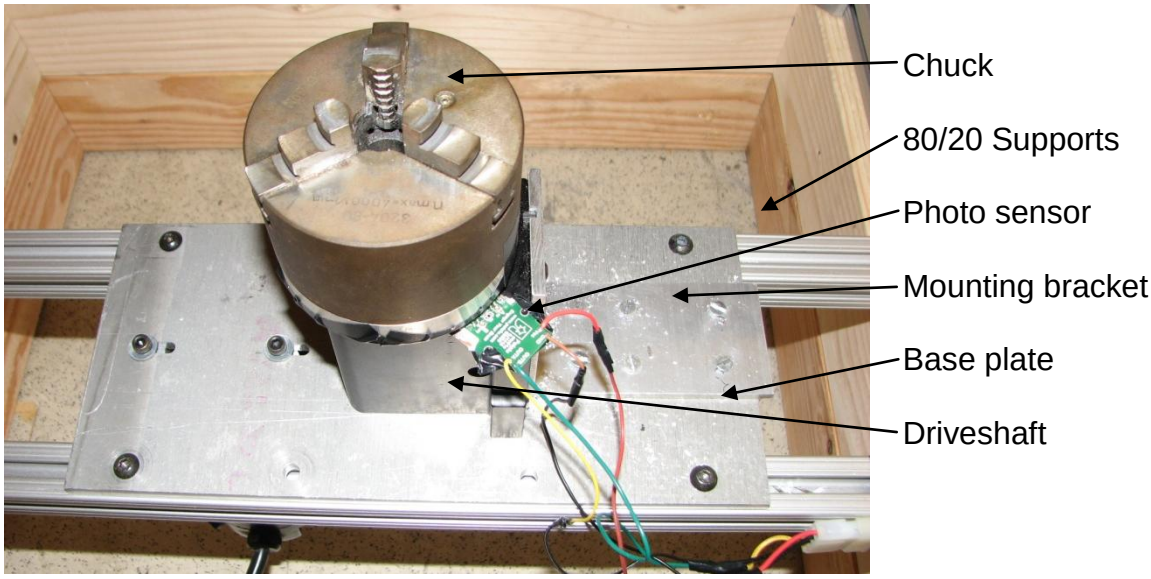

Figure 15: Picture showing the chuck and driveshaft with mounting and sensor.

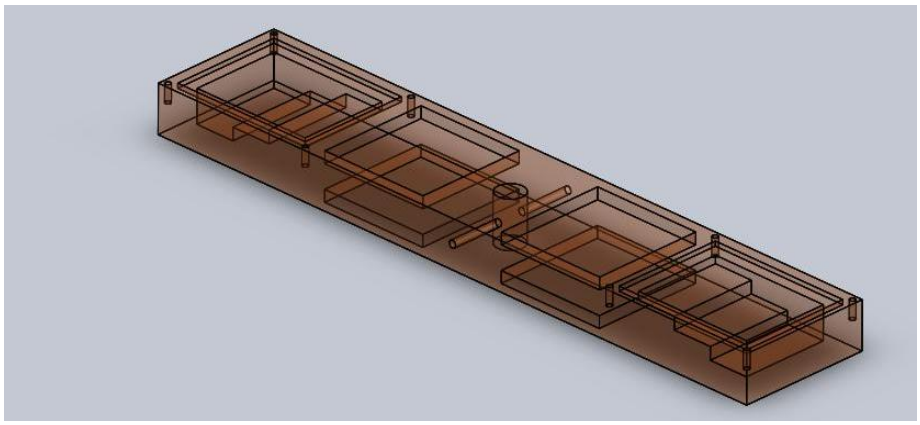

Figure 16: Centrifuge arm design. The centrifuge consists of two testing areas offering us 3 horizontal and 2 vertical testing areas per pocket. Additionally pocket was milled out toward the center of the bar to reduce its total mass. A hole for a locking pin is drilled into the center intersecting the axis of rotation.

www.manaraa.com

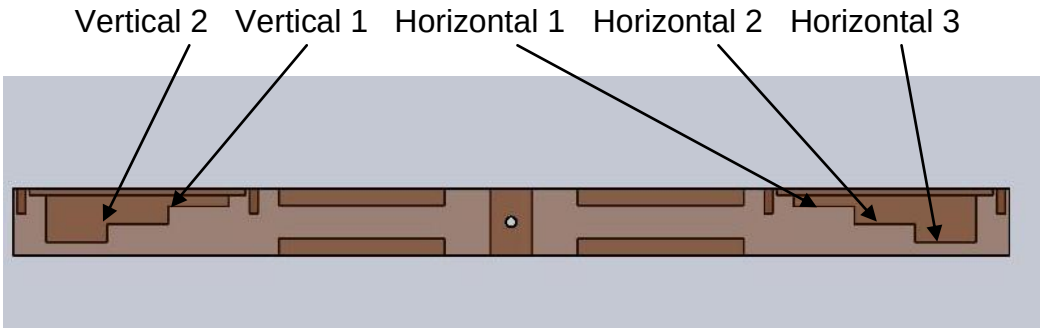

Figure 17: Cross sectional view of the centrifuge bar showing the different testing locations. Both vertical and horizontal sites exist in both sides of the bar though only one of each is labeled.

It was necessary to accurately measure the rotational speed of the arm in order to calculate the amount of force being seen by the parts. In order to do this an infrared emitter and detector were used. They were placed just behind the base of the chuck. To obtain the number of rotations the chuck made, all but a small part of the reflective aluminum was covered. The signal frequency was measured by an oscilloscope capable of giving the frequency readout (*f*). The oscilloscope used was a Tektronix TDS2002B. This frequency was then converted directly to acceleration by use of the centripetal acceleration formula,

$$a_c = \omega^2 r = (2\pi f)^2 \qquad (9).$$

www.manaraa.com

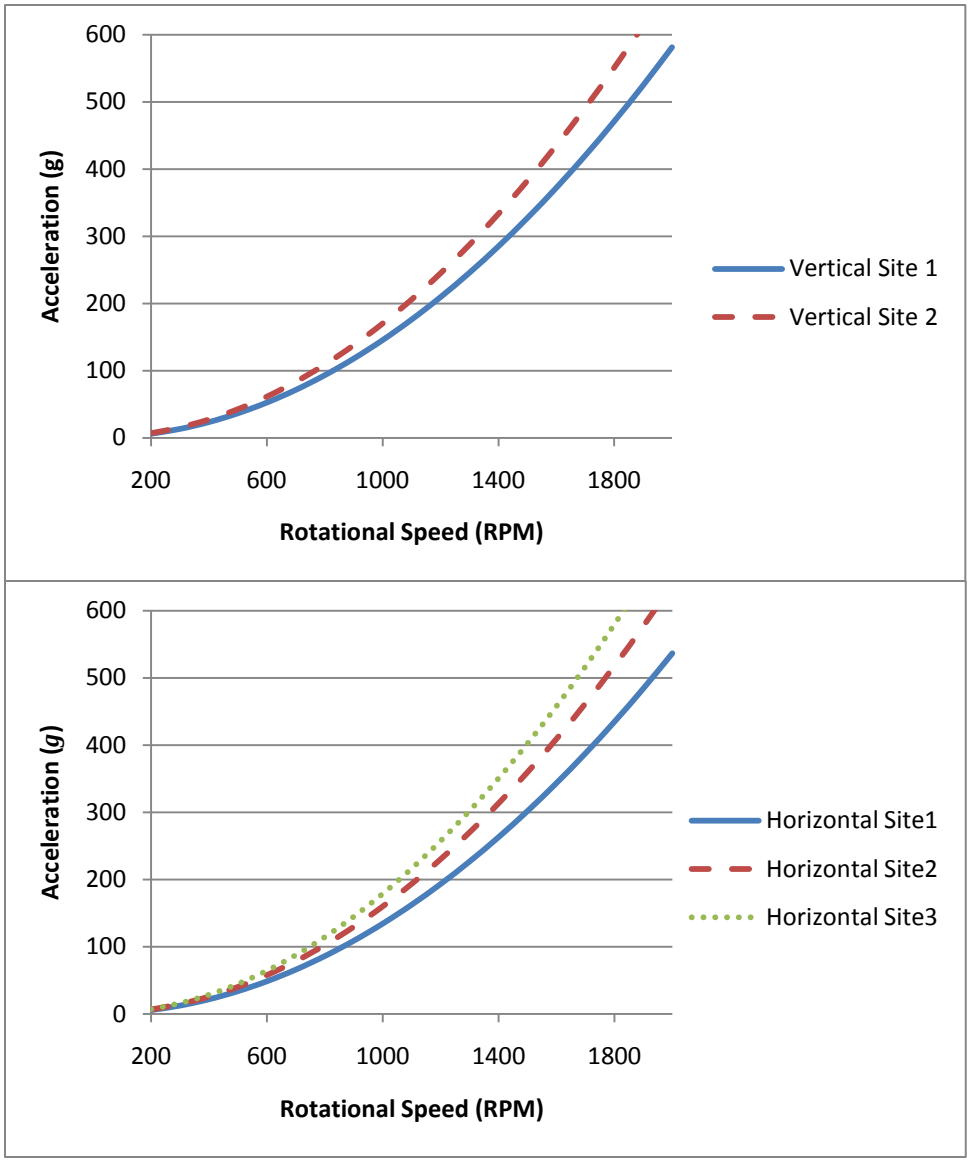

Figure 18: Graphs showing the g force experience by the parts at different testing locations over different speed ranges.

3.5.1 Fabrication of Centrifuge Test Sites

Additional sites needed to be made for centrifuge testing. The sites were made into strips with 6 solder bumps per strip and alignment marks were placed

www.manaraa.com

near each site so measurements could later be made. Each site had a tail which allowed them to be secured in the centrifuge holder while being tested. They were fabricated using the same method as the 0.025" assembly sites, using photolithography and E-beam deposition to create the copper regions. An additional step was added between the chromium and copper deposition masking the alignment lines to prevent deposition of copper onto them. The sites were fabricated on a 2" SiO_2 wafer and then diced into 1 x 6 arrays.

3.5.2 Centrifuge Experimental Process

In order to obtain data on the solder, it must be kept in its liquid state. A hot water bath large enough to accommodate the bar was used for this. The water was heated to 165 °F. A significantly higher temperature, than that of the solder melting point, was used because the bar experiences significant heat losses during spinning and lower temperature trials were found to be ineffective. The experimental trials were completed by first loading the samples to be tested into the bar parallel to the spinning axis, so that the centripetal force caused solder to come off the top of the sites toward the outside of the bar. The bar was preheated using a water bath, being careful to avoid contamination in the containment area. Once the samples were loaded in and the bar was preheated, DI water, heated to 165 °C or higher, was used to fill the pockets. A gasket was used to seal the containment area and a clear polypropylene window was screwed into place over the top to secure the holders and to make a water tight seal with the gasket. The innermost side of the seal was left without a screw on

www.manaraa.com

the center side to allow expanding gasses to escape during heating; this is not a problem because this side of the containment area sees no liquid during the testing. This process is performed on both containment areas so that balance of the bar is maintained. Once the containment areas were sealed off the bar was partially submerged in the hot water bath, a support was used to support the bar to prevent the submersion of the polypropylene covers and prevent unwanted contamination of the containment area. A surface temperature probe is used to monitor the temperature of the bar; when the bar had equilibrated to the water it was removed, dried and placed in the centrifuge for testing. The bar was slowly spun up until reaching the desired speed as measured by the oscilloscope.

3.5.3 Centrifuge Data Analysis

Analysis of the solder bumps tested in the centrifuge proved to be more difficult to acquire than originally anticipated. Several methods were considered for the task though in the end most proved incapable of the task. Weighing the parts seemed an obvious method to measure the amount of material removed during the testing. However, the option would have required us to make only one site per test strip and the weight of the solder removed compared to the total weight of the strips was relatively small making most of the results fall out of the range that could accurately be measured with the scale available. The second method considered was a 3D profilometry scan. The profilometer had a limitation of 280 microns in height, about half of the maximum height of some of the solder samples.

www.manaraa.com

The other technique considered was optical analysis. A goniometer with a digital camera was used to capture images of the drops. The disadvantage of this is that the exact volume of the drops remains unknown because only one face of the solder bump can be captured. However the drops can be assumed to be symmetric and therefore the volume has a direct relation the area seen on one face. Since the aim of the experimentation is to see if it is possible to remove solder from the sites and make them for uniform, analysis of the area will be sufficient to measure the samples.

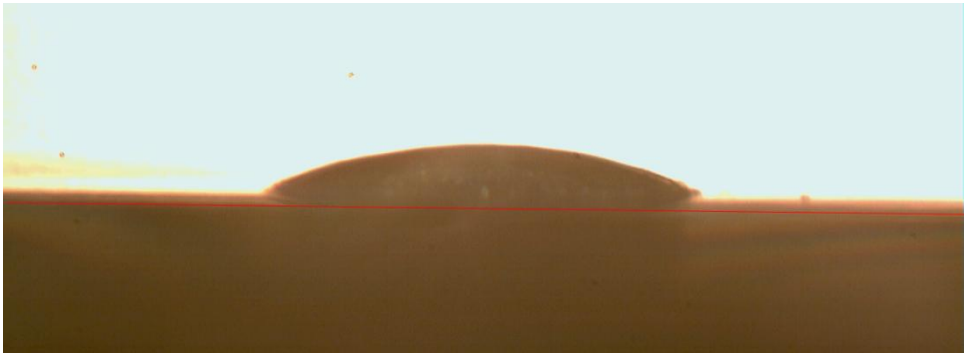

Figure 19: Sample of data acquired through goniometer.

The data for the solder bumps was acquired before and after their tests in the centrifuge. A position on the stage was marked and the focus was locked in place to ensure that the scaling of the samples would not change between measurements. One of the captured images can be seen in Figure 19. Once the photos had been acquired they were imported to Adobe® Photoshop® CS3. The base plane was defined with a contrasting colored line to prevent capturing it as part of the droplet. The software automatically selects the silhouette of the drop and it is able to record the height, width and area of the selection in pixels. The

www.manaraa.com

pixels are then converted to millimeters using the known length at the base of the drop as a reference. A large problem in the data analysis came from the copper sites dissolving into the solder bumps with extended exposure to the molten solder. An EDS spectrum analysis was performed to validate this conclusion. Looking at the images the most important things to note are that there is copper present in the solder bump area, indicating that it has absorbed some of the copper from the site. It can also be seen that areas without solder are devoid of copper and show large amounts of the silicon, the only other element present in these locations is a small layer of chromium. The results of pertinent element presences can be seen in Figure 20. The most important to note is the noticeable amount of silicon present in what should be a site entirely coated by solder.

www.manaraa.com

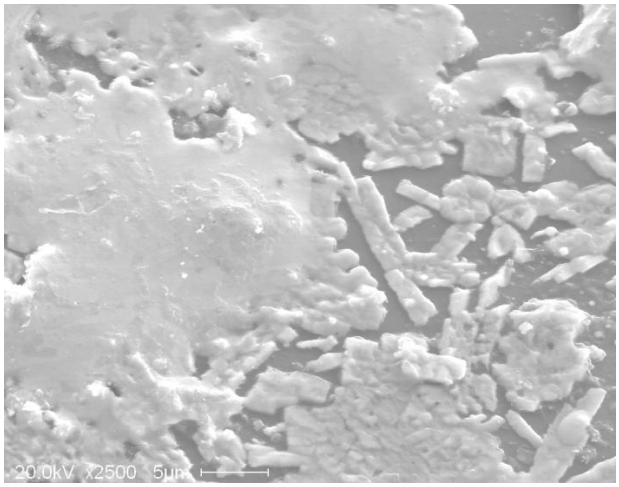

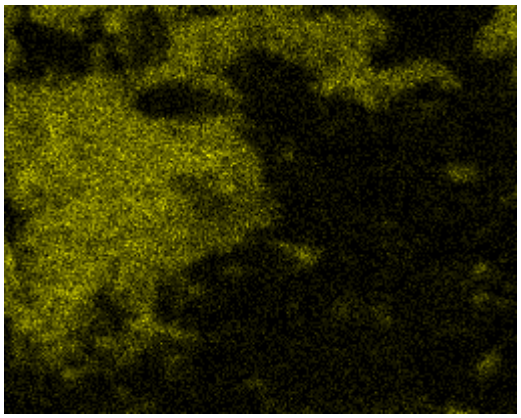

Bi

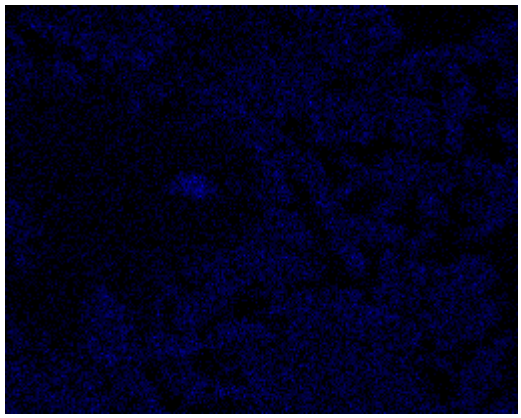

Cu

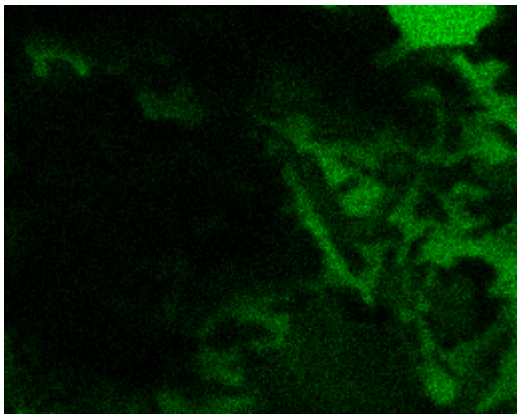

Si

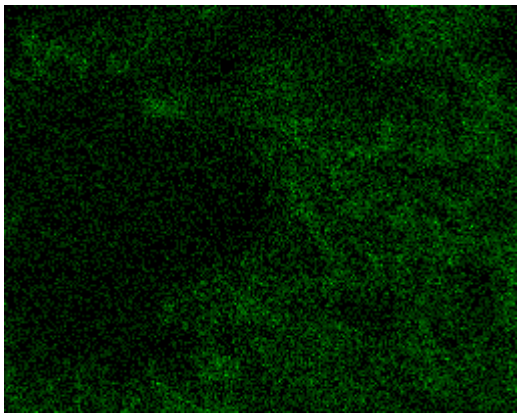

Cr

Figure 20: Spectrum analysis performed using EDAX system. The SEM image is shown at the top followed by the scans showing the presence of the indicated elements.

www.manaraa.com

The data was collected and the errors caused by the dissolving copper are evident. Many sites appear to have grown or show little change in volume. It is believed that some of these tests may not have been molten when they were spun based on the extreme change in some sites while there is almost none in the others. Only one size of sites shows a reduction in standard deviation. Statistical analysis is forgone because there is too much error from the changing site geometry to make any definite conclusions. As soon as sites can be fabricated with thicker metal layers the tests will be repeated, giving the sites more time before all copper would be absorbed by the solder. The raw data can be found in the appendices. From the data we can see that there is likely some error in the measurement despite efforts to standardize it. The only sites that did not experience significant pad size reductions are those that did not significantly change in volume. This suggests that all sites which were kept hot enough to be molten during the test also experienced the most diffusion of copper and subsequent pad size reduction. Observation of the tests suggested that spinning speed around 12-15Hz produced good results other than the aforementioned errors.

A plot of the data taken for samples spun in the centrifuge at a range of different speeds is shown in Figure 21. The location of the copper loss had significant effects on our measurement technique, because we were only capturing one face of the drop. If most of the absorption occurred in front or behind the site as we view it the amount of solder would appear to grow. Greater amounts of solder were lost from those experiencing absorption in the center of

www.manaraa.com

the site, this is likely due to the change in surface tension because of the significant change in shape of the drop caused by the absorption. Three distinct sets of data appear, those which failed to have any solder removed, or having the appearance of solder growth. This is due to the solder absorbing in the front and back of the site as described above. This group of samples, labeled C, is highlighted in red. A second smaller group of sites which were observed still be coated properly with a small amount of solder removed. This group, labeled B, is highlighted in blue. The last set of data, labeled A, is sites that which a large amount of solder removed, with significant site deterioration, as shown in the spectrum analysis of Figure 20. The speeds used to test these parts seemed promising for removing small amounts of solder if the issue of copper absorption by the solder can be addressed.

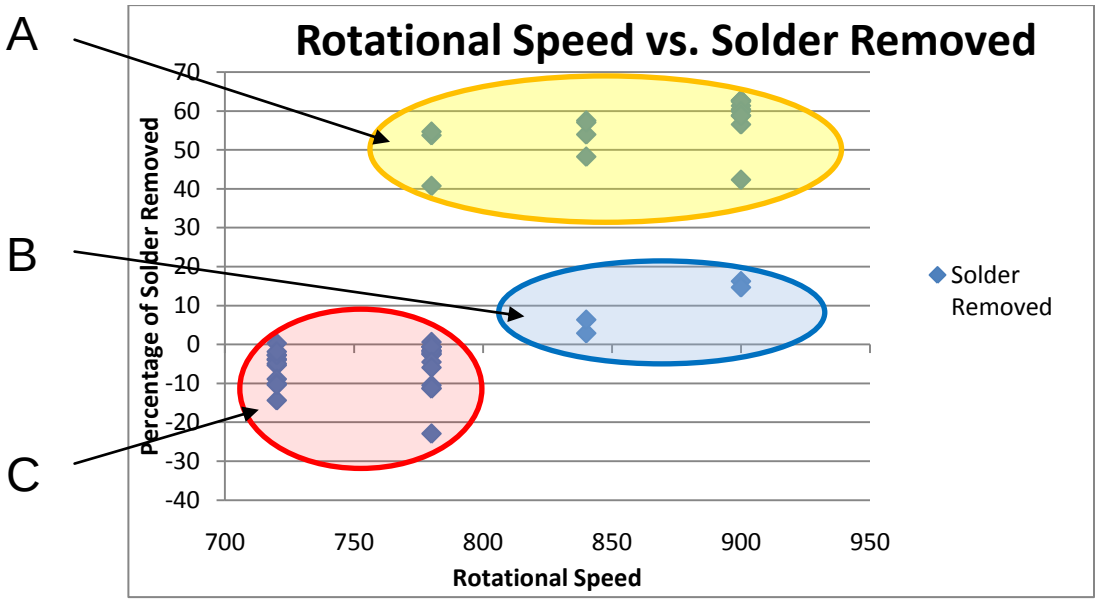

Figure 21: Graph of percentage of solder removed to the rotational speed of the centrifuge.

www.manaraa.com

Chapter 4 – Results and Conclusions

It has been successfully shown that thermoelectric elements of varying sizes can be assembled through the use of capillary self-assembly. Several problems have been tackled in the creation of these assemblies. The main problem was creating a process that could use the materials found commonly in the assembly of thermo electric coolers, without the destruction of these materials. Additional problems included the coating of substrates with solder, misalignment of parts during transfer and assembly and diffusion of metallic pads into solder alloys.

4.1 Assembly of TECs

We have successfully created TEC assemblies using the wafer to wafer transfer method outline by Crane *et al.* with some modification. Several parameters had to be fine tuned in order to reliably produce assemblies using this method. The pH of the solution had to be carefully controlled during the assembly and the application of solder to the sites. Too little acidity would result in a scenario where parts were unable to bond due to oxide layers formed on the outside of the solder. At the same time, too high acidity would corrode parts and sites before they had enough time to find a stable assembly site. The application of solder saw additional problems as several of the sites would often not wet the

www.manaraa.com

low melting alloys used in our experimentation. The application of ultrasonic vibration while the parts were in contact with the solder bath was found to greatly increase their consistency of the solder coatings.

During the assembly process some other minor adjustments were added. It was found that agitation forces should be directed such that parts are brought into contact with the sites. In the larger assemblies, this was accomplished by manual rotation and inspection of the parts so that they were continuously tumbled over the substrate. In the smaller assembly, the parts could easily be manipulated by use of a pipette. Numerous (10-50) parts could be caught up in the flow and deposited over the sites in one small squeeze of the pipette. The addition of a substrate holder for the transfer process was key to the alignment and successful transfer of the parts from the temporary substrates onto the final substrate and also in the final assembly step for completing the circuit of the TEC.

4.2 Centrifuge Data

The centrifuge provided a method of improving our assemblies by allowing us to expose the sites to acceleration. It is theorized that this will create more uniform sites. However, the diffusion of the copper sites into the solder seems to be a constant problem in centrifuge testing. This caused many of the testing sites to become useless for our data measurement. Therefore many of the testing sites did not contribute valuable data. In order to better assess the problems afflicting the sites, a spectrum analysis of the remaining material on one of the

www.manaraa.com

sites was performed. It was found that nothing but the chromium adhesion layer remained in many area meaning the solder must have absorbed it. Still there were some sites able to be processed without experiencing this diffusion to the point of destruction of the site. While the centrifuge tests may not have yielded the statistical evidence of the reduction in variation we were hoping for, it did offer valuable insight into the nature of the interaction of the solder and the metallic sites.

4.3 Future Work

While successful assemblies have been created several challenges remain to ultimately applying this process to large batches to produce commercial TECs. Primarily alignment errors need to be minimized in order to more closely pack the elements, thereby creating more efficient compact coolers. Additional testing with the centrifuge needs to be done to validate models established in prior works. Additionally thicker metallic sites need to be fabricated so that the solder uniformity tests can be repeated without having to worry about the copper diffusion.

Futures TEC assemblies will involve even smaller parts. Already a mask has been developed for assemblies of 0.012 x 0.012” elements. As assemblies decrease in size the efficiency of the TEC should greatly increase. In order to help in fabricating working TECs in this size scale where checking each individual site can be difficult a redundancy is used. This places two parts in

www.manaraa.com

parallel at every site instead of one. In this method, one of the parts could be missing without causing an open circuit in the device as shown in Figure 22.

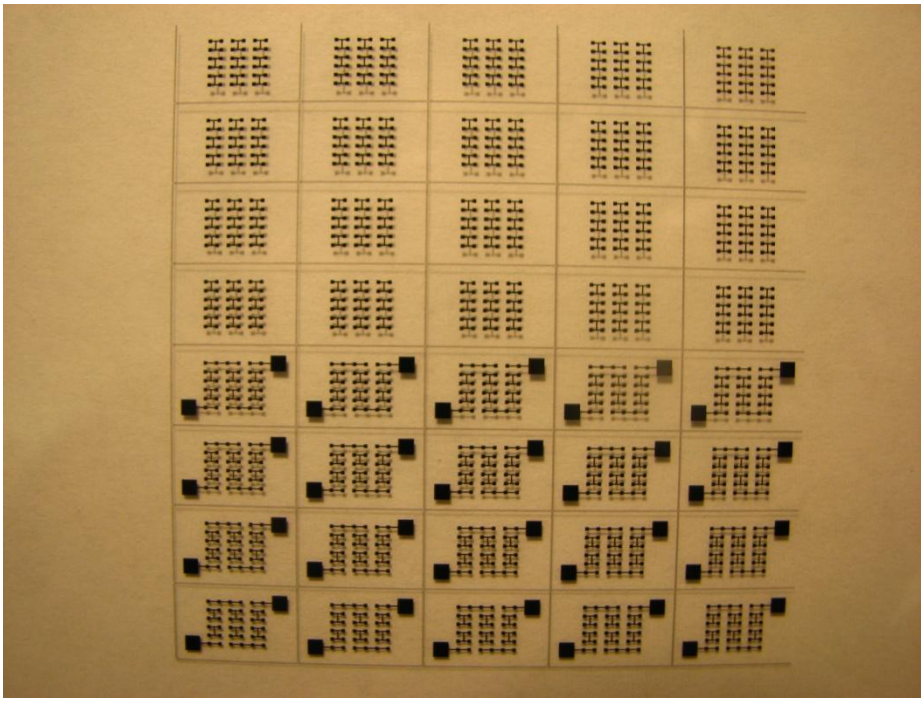

Figure 22: Mask for future TEC assembly of 0.012 x 0.012” elements. The mask features redundant sites to aid in successful cooler assembly.

www.manaraa.com

List of References

[1] Li, D., 2005, "Thermal Transport in Nanostructured Solid-State Cooling Devices," Journal of Heat Transfer, 127(1) pp. 108-114.

[2] Miner, A., 2007, "The Compatibility of Thin Films and Nanostructures in Thermoelectric Cooling Systems," Journal of Heat Transfer, pp. 12.

[3] Srinivasan, U., 2001, "Microstructure to Substrate Self-Assembly using Capillary Forces," Journal of Microelectromechanical Systems, 10(1) pp. 17.

[4] Srinivasan, U., 2002, "MEMS: Some Self-Assembly Required," Optics and Photonics News, 13(11) pp. 20.

[5] Whitesides, G., 2002, "Self-Assembly at all Scales," Science, 295(5564) pp. 2418-2421.

[6] Crane, N., 2009, "Self-Assembly for Integration of Microscale Thermoelectric Coolers," Journal of Electronic Materials, 38(7) pp. 1252.

[7] Brady, G.S., Brady, G.S.b., and Clauser, H.R., 1929, "Materials handbook," McGraw-Hill Book Co., New York, .

[8] Goldsmid, H.J., 1964, "Thermoelectric refrigeration," Plenum Press, New York, pp. 240.

[9] Pelesko, J.A., 2007, "Self assembly: the science of things that put themselves together," CRC Press, .

[10] Zheng, W., 2005, "Non-Robotic Fabrication of Packaged Microsystems by Shape-and-Solder- Directed Self-Assembly," Proceedings of the IEEE International Conference on Micro Electro Mechanical Systems (MEMS), pp. 8.

[11] Tien, J., 1997, "Microfabrication through Electrostatic Self-Assembly," Langmuir, 13(20) pp. 5349.

[12] Singamaneni, S., 2005, "Fabrication of Ni Nanoparticles and their Size-Selective Self-Assembly into Chains Under External Magnetic Field," Applied Physics Letters, 87(16) pp. 1-3.

www.manaraa.com

[13] Nakakubo, T., 2000, "Three-Dimensional Micro Self-Assembly using Bridging Flocculation," Sensors and Actuators.A, Physical, 83(1) pp. 161-166.

[14] Yeh, H., 1994, "Fluidic Self-Assembly for the Integration of GaAs Light-Emitting Diodes on Si Substrates," IEEE Photonics Technology Letters, 6(6) pp. 706.

[15] Bishop, K. J. M., 2009, "Nanoscale Forces and their Uses in Self-Assembly," Small, 5(14) pp. 1600-1630.

[16] Philp, D., and Stoddart, J. F., 1996, "Self-Assembly in Natural and Unnatural Systems," Angewandte Chemie International Edition in English, 35(11) pp. 1154-1196.

[17] Desiraju, G. R., 1995, "Supramolecular Synthons in Crystal Engineering?A New Organic Synthesis," Angewandte Chemie International Edition in English, 34(21) pp. 2311-2327.

[18] Lehn, J. -., 1990, "Perspectives in Supramolecular Chemistry?from Molecular Recognition Towards Molecular Information Processing and Self-Organization," Angewandte Chemie International Edition in English, 29(11) pp. 1304-1319.

[19] Milner, S. T., 1991, "Polymer Brushes," Science, 251(4996) pp. pp. 905-914.

[20] Smith, J. S., 2000, "High Density, Low Parasitic Direct Integration by Fluidic Self Assembly (FSA)," Technical Digest - International Electron Devices Meeting, ISSU(PAGE) pp. 201-204.

[21] Lienemann, J., Greiner, A., Korvink, J. G., 2003, "Modeling, Simulation, and Experimentation of a Promising New Packaging Technology: Parallel Fluidic Self-Assembly of Microdevices," Sensors Update, 13(1) pp. 3-43.

[22] Ramadoss, V., 2008, "Analysis of capillary forces in electrowetting and precision self assembly [electronic resource]," University of South Florida, Tampa, Fla, .

[23] Srinivasan, U., 2002, "Fluidic Self-Assembly of Micromirrors Onto Microactuators using Capillary Forces," IEEE Journal of Selected Topics in Quantum Electronics, 8(1) pp. 4.

[24] Greiner, A., 2002, "Capillary forces in micro-fluidic self-assembly," .

www.manaraa.com

[25] Bohringer, K. F., Srinivasan, U., and Howe, R. T., 2001, "Modeling of capillary forces and binding sites for fluidic self-assembly," Micro Electro Mechanical Systems, 2001. MEMS 2001. The 14th IEEE International Conference on, Anonymous pp. 369-374.

[26] Andreas, T., 1997, "Three-Dimensional Self-Assembly of Millimetre-Scale Components," Nature, 386(6621) pp. 162-164.

[27] Xiong, X., 2003, "Controlled Multibatch Self-Assembly of Microdevices," Journal of Microelectromechanical Systems, 12(2) pp. 117.

[28] Singh, B. P., Onozawa, K., Yamanaka, K., AUG, 2005, "Novel High Precision Optoelectronic Device Fabrication Technique using Guided Fluidic Assembly," The Optical Society of Japan, 12pp. 345.

[29] Fang, J., and Bohringer, K. F., 2006, "Parallel Micro Component-to-Substrate Assembly with Controlled Poses and High Surface Coverage," Journal of Micromechanics and Microengineering, 16(4) pp. 721-730.

[30] Scott, K., 2004, "High-Performance Inductors using Capillary Based Fluidic Self-Assembly," Journal of Microelectromechanical Systems, 13(2) pp. 300.

[31] Green, P. W., 1995, "Demonstration of Three-Dimensional Microstructure Self-Assembly," Journal of Microelectromechanical Systems, 4(4) pp. 170-175.

[32] Cannon, A. H., Hua, Y., Henderson, C. L., 2005, "Self-Assembly for Three-Dimensional Integration of Functional Electrical Components," Journal of Micromechanics and Microengineering, 15(11) pp. 2172-2178.

[33] Gracias, D., 2000, "Forming Electrical Networks in Three Dimensions by Self-Assembly," Science, 289(5482) pp. 1170.

[34] Van Schuylenbergh, K., 2002, "Self-Assembled Out-of-Plane High-Q Integrated Inductors," Technical Digest - International Electron Devices Meeting, ISSU(PAGE) pp. 479-482.

[35] Jacobs, H., 2002, "Fabrication of a Cylindrical Display by Patterned Assembly," Science, 296(5566) pp. 323-325.

[36] Zheng, W., Buhlmann, P., and Jacobs, H. O., 2004, "Sequential Shape-and-Solder-Directed Self-Assembly of Functional Microsystems," Proceedings of the National Academy of Sciences of the United States of America, 101(35) pp. 12814-12817.

www.manaraa.com

[37] Zheng, W., 2006, "Self-Assembly Process to Integrate and Connect Semiconductor Dies on Surfaces with Single-Angular Orientation and Contact-Pad Registration," Advanced Materials, 18(11) pp. 1387.

[38] S.A. Stauth, and B.A. Parviz, 2006, "Modeling of Fluidic Self-Assembly for Integration of Silicon Components on Plastic," Micro Electro Mechanical Systems, 2006. MEMS 2006 Istanbul. 19th IEEE International Conference on, pp. 194-197.

[39] Syms, R. R. A., 1993, "Self-Assembly of Three-Dimensional Microstructures using Rotation by Surface Tension Forces," Electronics Letters, 29(8) pp. 662-664.

[40] Syms, R. R. A., 1995, "Equilibrium of Hinged and Hingeless Structures Rotated using Surface Tension Forces," Journal of Microelectromechanical Systems, 4(4) pp. 177-184.

[41] Lin, W., 1995, "Design of Solder Joints for Self-Aligned Optoelectronic Assemblies," IEEE Transactions on Components, Packaging, and Manufacturing Technology.Part B, Advanced Packaging, 18(3) pp. 543-551.

[42] Su, B., 1997, "Gas Flow Effects on Precision Solder Self-Alignment," Proceedings - Electronic Components and Technology Conference, ISSU(PAGE) pp. 797-803.

[43] Jairazbhoy, V., 1996, "Prediction of Equilibrium Shapes and Pedestal Heights of Solder Joints for Leadless Chip Components," IEEE Transactions on Components, Packaging, and Manufacturing Technology.Part A, 19(2) pp. 224.

[44] Harsh, K., 1999, "Solder Self-Assembly for Three-Dimensional Microelectromechanical Systems," Sensors and Actuators.A, Physical, 77(3) pp. 237-244.

[45] McCarthy, B., 2003, "A Multi-Component Solder Self-Assembled Micromirror," Sensors and Actuators.A, Physical, 103(1-2) pp. 187-193.

[46] Shet, S., 2004, "The Magnetic Field-Assisted Assembly of Nanoscale Semiconductor Devices: A New Technique," JOM, 56(10) pp. 32.

[47] Choi, Y., 2005, "Biochip microarray using magnetic force interaction and self-assembly," .

[48] Shetye, S., 2010, "Magnetic Self-Assembly of Millimeter-Scale Components with Angular Orientation," Journal of Microelectromechanical Systems, 19(3) pp. 599-609.

www.manaraa.com

[49] Harsh, K. F., Kladitis, P. E., Zhang, Y., 2000, "Tolerance and Precision Study for Solder Self-Assembled MEMS," Proceedings of SPIE--the International Society for Optical Engineering, 4075pp. 173-184.

[50] Norton, R.L., 2006, "Machine design : an integrated approach," Pearson Prentice Hall, Upper Saddle River, N.J., pp. 984.

www.manaraa.com

Appendices

www.manaraa.com

Appendix A – Raw Centrifuge Data

Document	Width	Pad Size	Width 2	Area1 mm^2	Area2 mm^2	delta
strip1bump1	638	1	632	0.1392878	0.14477297	-0.00549
strip1bump2	645	1	636	0.1566645	0.16096621	-0.0043
strip1bump3	651	1	642	0.1601371	0.16609466	-0.00596
strip1bump4	623	1	640	0.1384965	0.14584544	-0.00735
strip1bump5	640	1	630	0.1274813	0.13372945	-0.00625
strip1bump6	650	1	642	0.1306585	0.142243	-0.01158
strip2bump1	656	1	644	0.1310507	0.1441895	-0.01314
strip2bump2	646	1	644	0.1384941	0.15835828	-0.01986
strip2bump3	646	1	654	0.2101861	0.21576337	-0.00558
strip2bump4	650	1	637	0.1543448	0.17031128	-0.01597
strip2bump5	648	1	642	0.1657191	0.16518755	0.000532
strip2bump6	652	1	654	0.1946496	0.19820475	-0.00356
strip3bump1	660	1	658	0.2055348	0.21069634	-0.00516
strip3bump2	648	1	644	0.1379508	0.14120125	-0.00325
strip3bump3	648	1	652	0.1704908	0.16939709	0.001094
strip3bump4	652	1	654	0.2488562	0.25364208	-0.00479
strip3bump5	638	1	648	0.1244529	0.12516156	-0.00071
strip3bump6	651	1	650	0.2511924	0.25524841	-0.00406
			STD DEV	0.0401688	0.0389447	0.001224
strip4bump1	716	1.1	708	0.2921539	0.13502632	0.157128
strip4bump2	718	1.1	720	0.2388189	0.24031189	-0.00149
strip4bump3	714	1.1	698	0.2327905	0.10542258	0.127368
strip4bump4	716	1.1	714	0.2052797	0.20838369	-0.0031
strip4bump5	718	1.1	714	0.1899841	0.19107547	-0.00109
strip4bump6	708	1.1	722	0.1839958	0.19227077	-0.00827
strip5bump1	713	1.1	690	0.1861289	0.09625704	0.089872
strip5bump2	728	1.1	704	0.2312834	0.10640291	0.12488
strip5bump3	726	1.1	716	0.2295873	0.09743108	0.132156
strip5bump4	714	1.1	714	0.2097113	0.20360013	0.006111
strip5bump5	720	1.1	688	0.2475144	0.10616905	0.141345
strip5bump6	723	1.1	706	0.2028844	0.18995104	0.012933
strip7bump1	742	1.1	682	0.2039639	0.07592278	0.128041
strip7bump2	725	1.1	692	0.1897384	0.15886617	0.030872

المنارة للاستشارات
www.manaraa.com

Appendix A (Continued)

strip7bump4	731	1.1	528	0.1967614	0.07339281	0.123369
strip7bump5	716	1.1	664	0.2128743	0.09244201	0.120432
strip7bump6	728	1.1	533	0.1750925	0.06922579	0.105867
strip8bump1	736	1.1	668	0.3374477	0.13035143	0.207096
strip8bump2	739	1.1	665	0.2729582	0.10249339	0.170465
strip8bump3	748	1.1	677	0.2435482	0.09759644	0.145952
strip8bump4	706	1.1	670	0.2150641	0.08837657	0.126688
strip8bump5	723	1.1	680	0.244949	0.1010217	0.143927
strip8bump6	722	1.1	668	0.2322802	0.13390189	0.098378
			STD DEV	0.0384999	0.04922537	-0.01073
strip6bump1	590	0.9	557	0.1154338	0.0683683	0.047066
strip6bump2	558	0.9	558	0.0797047	0.09794369	-0.01824
strip6bump3	572	0.9	568	0.1058856	0.11696927	-0.01108
strip6bump4	570	0.9	578	0.0941263	0.10476115	-0.01063
strip6bump5	574	0.9	570	0.1090912	0.11553302	-0.00644
strip6bump6	582	0.9	562	0.1059801	0.11788582	-0.01191
			STD DEV	0.0128081	0.01897277	-0.00616

www.manaraa.com